1   Manuscript type: Research article

2   Assessing Landslide Damming susceptibility in Central Asia

3   Carlo Tacconi Stefanelli[a,b,*], William Frodella[a,b], Francesco Caleca[a,b], Zhanar Raimbekova[c],

4   Ruslan Umuraliev[d], Veronica Tofani[a,b]

5   [a] University of Florence, Department of Earth Sciences, via G. la Pira 4, 50121 Florence, Italy

6   [b] UNESCO Chair on the Prevention and Sustainable Management of Geo-Hydrological Hazards, University of

7   Florence, Largo Fermi 2, 50125 Florence, Italy

8   [c] Institute of Seismology of Republic of Kazakhstan (IS), Almaty, Kazakhstan

9   [d] Institute of Seismology of the National Academy of Sciences of Kyrgyz Republic (ISNASKR), Bishkek, Kyrgyz

10   Republic

11   *   *Correspondence to*: carlo.tacconistefanelli@unifi.it

12   **Abstract**

13   Central Asia regions are characterized by active tectonics, high mountain chains with extreme topography with

14   glaciers and strong seasonal rainfall events. These key predisposing factors make large landslides a serious natural

15   threat in the area, causing several casualties every year. The mountain crests are divided by wide lenticular or

16   narrow, linear intermountain tectonic depressions, which are incised by many of the most important Central Asia

17   rivers and are also subject to major seasonal river flood hazard. This multi-hazard combination is a source of

18   potential damming scenarios which can bring cascading effects with devastating consequences for the surrounding

19   settlements and population. Different hazards can only be managed with a multi-hazard approach coherent within

20   the different countries, as suggested by the requirements of the Sendai Framework for Disaster Risk Reduction.

21   This work was carried out within the framework of the SFRARR Project ("*Strengthening Financial Resilience*

22   *and Accelerating Risk Reduction in Central Asia*") as a part of a multi-hazard approach with the aim of providing

23   a damming susceptibility analysis at a regional scale for Central Asia. To achieve this, a semi-automated GIS-

24   based mapping method, centred on a bivariate correlation of morphometric parameters defined by a morphological

25   index, originally designed to assess the damming susceptibility at basin/regional scale, was modified to be adopted

26   nationwide and applied to spatially assess the obstruction of the river network in Central Asia for mapped and

27   newly formed landslides. The proposed methodology represents an improvement of the previously designed,

28   requiring a smaller amount of data, bringing new information on the damming hazard management and risk

29   reduction for the Central Asia regions.

30   **1   Introduction**

31   The mountainous areas of the Djungaria, Tien Shan, Pamir and Kopetdag in Central Asia territories are

32   characterized by complex and active tectonic and are the sources of most of Central Asia rivers. A rugged

33   topography along with complex geological structure and high seismicity are ideal setting for large slope failures.

34   In general, when landslides completely obstruct a river channel, they generate a landslide dam whose consequences

35   can be a serious hazard forming upstream backwater and causing catastrophic downstream flooding, changes in

36   the riverbed course, embankments instability triggering other landslides with a cascading effect (Swanson et al.

37   1986; Costa and Schuster 1988; Casagli and Ermini 1999). The effects of impounded water and anomalous flood

38   waves, resulting from a dam breach, have significant economic and social impacts in upstream and downstream

39   areas with economic and human losses (King et al. 1989; Dai et al. 2005; Chen and Chang 2016). Rebuilding costs

40   can be extensive, as they are direct (e.g., infrastructure and buildings reconstruction, safety measures) and indirect

41   (e.g., loss in real estate value and damage caused to industrial and agricultural production), harder to estimate.

42   Most of landslide dams have a short life as about 40% of them collapse within 24 hours after formation and about

43   80% within one year (Tacconi Stefanelli et al, 2015; Fan et al., 2020). Given the limited available time, a complete

44   and reliable analysis of the risks, requiring in-depth study of the phenomenon, is not achievable during the event

45   and only rapid assessments for the dam stability are suitable. When the people to evacuate are too many or the

46   related risk is too high, engineering measures for the hazard reduction are attempted: among these are for example

47   modification of slope geometry, drainage, retaining structures and internal slope reinforcement (Popescu and

48   Sasahara 2009; Schuster and Evans 2011). Therefore, part of the effects from landslide damming can be avoided

49   or at least reduced thanks to mitigation and prevention measures (e.g., slopes stabilization or re-profiling) if the

50   most critical areas with the highest damming probability are known. Consequently, planning and prevention tools,

51   such as risk and susceptibility mapping, are essential to reduce the costs of natural hazard and improve the

52   efficiency of environmental management.

53   Reactivation of ancient landslides triggered during different climatic and environmental conditions may often

54   generate new mass movements (Casagli and Ermini 1999; Canuti et al. 2004; Dikau and Schrott 1999; Borgatti

55   and Soldati 2010; Crozier 2010). Landslides generated in the past are now dormant, with strength parameters of

56   the sliding surface close to the residual ones, and difficult to recognize because vegetation, erosion and superficial

57   alteration hide their morphology. Natural causes, such as earthquakes, river undercutting, rainfall, and snowmelt,

58   or even anthropic activity can reactivate these ancient phenomena. Therefore, all dormant landslides capable to

59   reach a river along their pathway can potentially dam it and should be investigated. New landslides, instead, may

60   develop wherever are present suitable conditions along the slopes. The spatial occurrence probability is commonly

61   assessed by landslide susceptibility analysis, highly dependent on landslide volume (Catani et al., 2016), which is

62   difficult to accurately predict.

63   Landslides in Central Asia are quite common and a considerable number of them have huge dimension, often

64   induced by strong earthquakes but also by floods, heavy rainfall and snowmelt (Behling et al., 2014; Golovko,

65   2015; Havenith et al., 2015a, 2015b, 2006b; Kalmetieva et al., 2009; Rosi et al., 2023; Saponaro et al., 2014; Strom

66   and Abdrakhmatov, 2017, 2018). Concerning landslide dam events, in Central Asia regions several mass

67   movements of considerable size produced the obstruction of a river section, of which more than 100 still are

68   existing with a lake (Strom, 2010). Although many of these could be considered stable (Strom, 2010), the

69   occurrence of devastating outburst floods in the last century show that their potential hazard should never be

70   overlooked also considering the seismicity of the region. In the Rushan and Murgab districts of Gorno-Badakhshan

71   Autonomous Oblast (Pamirs, Tajikistan) along the Murghab river, the Usoi dam is one of the most famous of the

72   many cases in the regions. Its impounded lake, called Lake Sarez, is 60 km long with 500 m of depth and has a

73   stored volume of about 17 km³, representing the world deepest landslide-dammed lake (Costa and Schuster, 1991;

74   Fan et al., 2020). It was originated on February 18th, 1911, when a MW 7.2 earthquake triggered a giant wedge-

75   failure of about 2.2 km³ of rock (mainly quartzite, schist, shale and dolomite) and debris that blocked the Murgab

76   River and a tributary valley, forming the 560 m high, 5 km long and 4 km wide Usoi dam, impounding Lake Sarez,

77   also creating the smaller Lake Shadau (Strom, 2010).

78   Landslide dam evolution, according to some studies (Swanson et al. 1986; Ermini and Casagli, 2003; Dal Sasso et

79   al. 2014; Tacconi Stefanelli et al. 2016), can be estimated through geomorphological indexes which require

80   parameters characterizing the landslide (or the dam) and the river (or the lake). Geomorphological indexes are a

81   powerful classification tool, but their prediction power depend mainly on long studies, a large amount of data and

82   measurement efforts given their empirical nature. Many of these indexes need parameters not always available and

83   easy to acquire, such as grain size distribution (Liao et al. 2022) or landslide velocity (Swanson et al., 1986).

84   In this work, we propose a simple semi-automatic GIS-based mapping methodology to verify the damming

85   susceptibility of river networks at national scale from existing and neo-formed landslides trough a

86   geomorphological index. This activity research was carried out in the framework of the SFRARR Project

87   ("*Strengthening Financial Resilience and Accelerating Risk Reduction in Central Asia*") as a part of a multi-hazard

88   approach (Bazzurro et al., 2023).

89   The proposed mapping methodology represents an innovation in terms of application simplicity, availability of

90   data and of extension of the analysed area, bringing new information on the damming hazard in the Central Asia

91   regions where the landslide susceptibility is quite high (Rosi et al., 2023) and a set of input data required for the

92   methodology application were available.

93   **2   Study area**

94   Central Asia is a region of vast diversity encompassing high mountain chains, deserts, and steppes (Figure 1). The

95   southern and eastern parts of the region are predominantly occupied by the mountainous areas of Djungaria, Tien

96   Shan, Pamir, Kopetdag, and a small part of Western Altaj, with peaks exceeding 7,000 m above sea level (a.s.l)

97   (Strom, 2010). These intraplate mountain systems, developed in the Cenozoic as a result of the India-Asian

98   collision, is located between the Tarim Basin and the Kazakh Shield (Molnar and Tapponier 1975, Abdrakhmatov

99   et al., 1996; 2003; Zubovich et al., 2010, Ullah et al., 2015). This study focusses the attention on the territories of

100   Central Asia that includes Turkmenistan, Kazakhstan, Kyrgyz Republic, Uzbekistan, and Tajikistan, covering a

101   surface of more than $4 \cdot 10^6$ km². Mountain building began in the Oligocene (Chedia 1980) or later (Abdrakhmatov

102   et al. 1996), resulting in a complex system of basement folds interrupted by several thrusts and reverse faults with

103   lateral offset of important amounts (Delvaux et al. 2001).

Natural Hazards
and Earth System
Sciences
Discussions

Open Access

EGU
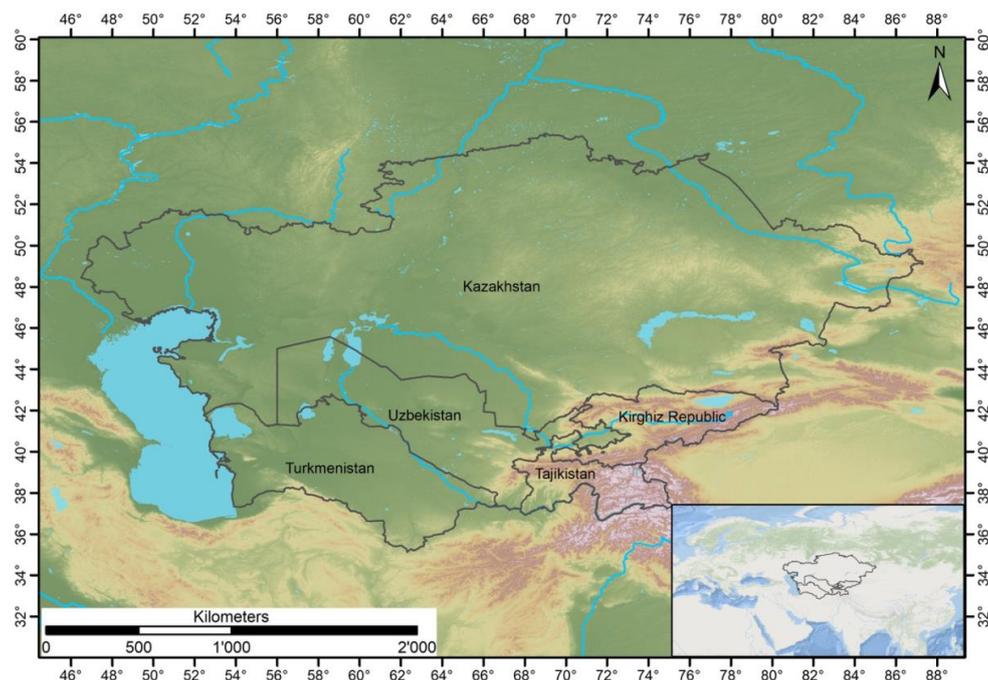
Figure 1. Geographical and geomorphological framework of the study area. Lake's polygons from Esri, Garmin International, Inc.; topographic base from NASA's SRTM project (Far and Kobrick, 2000).

The mountain belts contain several regional fault zones, and others cross the mountain systems with a NW-SE axis (Trifonov et al. 1992). Paleozoic crystalline rocks form, for the most part, the mountain ridges which correspond to a neotectonic anticline and are separated by tectonic depressions, with lenticular or linear shapes. These intermountain depressions host the primary river valleys and are filled by Neogene and Quaternary deposits, principally sandstone, siltstone interbedded by gypsum, and conglomerates (Strom and Abdrakhmatov, 2017). Lithologies from Mesozoic and Paleogene are characteristic of the areas at the foot of mountain ranges. This main deeply incised river network, fed by glaciers, snowmelt water and rain, is linked by narrow deep gorges up to 1-2 km deep (Strom and Abdrakhmatov, 2018) and is the origin of most of the rivers in Central Asia.

The retreat and shrinkage of glaciers in Central Asia regions induced by the global warming produce a seasonal variation in river discharge and consequently an increase of its induced hazards such as glacial lake outburst floods (GLOFs), resulting in countless losses of human life and destroyed infrastructure (Petrov et al. 2017; Wang et al., 2013). The high seismicity, frequent floods and a complex geological and topographical structure contribute to predispose the region to frequent landslides which can potentially obstruct the narrow valleys of the mountain ranges and in turn be the cause of chain risks (CAC DRMI, 2009; Havenit et al, 2017).

3   Materials and Methods

The Morphological Obstruction Index (MOI) (Tacconi Stefanelli et al., 2016) is a bivariate index able to evaluate the potential hazard posed by landslide dams that requires only simple morphometrical parameters which are easily extracted from common Digital Elevation Models. The MOI has been used in several studies, such as in Italy and Peru (Tacconi Stefanelli et al., 2016; 2018), to assess landslide damming susceptibility showing better results than others popular indexes (Swanson et al., 1986). It is a useful tool for identifying high-risk areas and for prioritizing mitigation efforts in landslide-prone regions.

The MOI is calculated by dividing the volume of the landslide, V_l (m³), by the width of the river valley, W_v (m), at the dam location.

$$MOI = log\left(V_l / W_v\right) \tag{1}$$

The MOI is based on the principle that the higher the ratio of the landslide volume to the river width, the greater the potential for dam formation. It is important to point out that river width, W_v, shall be defined as the width of the river valley which can potentially be obstructed creating a dammed lake and not of just the channel where the river flaws, as is often misinterpreted, although in narrow mountain valleys these often coincide.

Landslide dams analyzed by the index can be grouped within three evolutionary classes: formed, not formed and of uncertain evolution. The limits of these domains are depicted by two lines, the lower red "Non-formation line" and the upper blue "Formation line" (Figure 2).
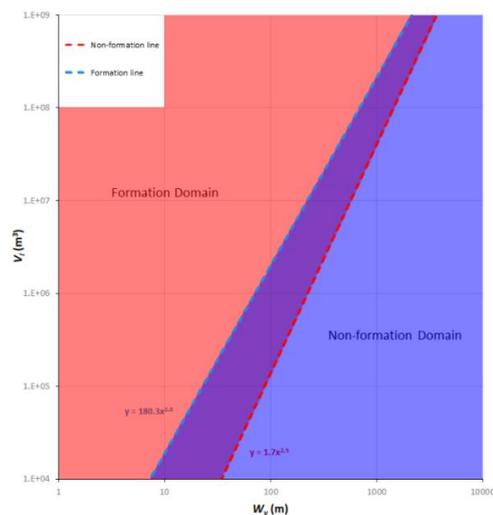
Figure 2. Schematic plot of the non-Formation line and Formation line.

The equation of the former is expressed as follows:

$$V_l' = 1.7 \cdot W_v^{2.5} \tag{2}$$

142   Where V_l' is the "Non-formation volume" and is the minimum landslide volume able to potentially block a river

143   with a given width W_v. Smaller volumes cannot completely dam the river. The latter expression draws the upper

144   limit for not formed dams and is expressed as follows:

145    $$V_l'' = 180.3 \cdot W_v^2$$ (3)

146   Where V_l'' is the "Formation volume", is the minimum landslide volume able to dam the river valley, with a

147   confidence of 99%, and the inferior boundary of the Formation domain (which includes only formed dams).

148   As originally proposed by Tacconi Stefanelli et al. (2020), these two equations, Eq.(2) and (3), can be used to

149   apply a simple semi-automatic methodology in order to verify at basin scale the damming susceptibility from

150   existing and neo-formed landslides. The following semi-automated procedure, inspired by the one of Tacconi

151   Stefanelli et al. (2020) of which this represents an improvement, is applied on a national scale and can be

152   reproduced entirely in a GIS (Geographic Information System) environment.

153   Within an even medium-long time interval the valley width in each river stretch does not change significantly and

154   can be considered an immutable factor in the MOI equation (Eq.(1)). Starting from this assumption, along with

155   Eq. (2) and Eq. (3), if the average river width W_v of each river stretch can be assessed, the two threshold landslide

156   volumes V_l' (Non-formation volume) and V_l'' (Formation volume) can be estimated for each river stretch.

157   Landslides that cause river obstruction are in many cases reactivations of ancient movements that are still in a

158   condition of partial instability and that have not reached a potential equilibrium reaching the valley floor.

159   Therefore, with a landslide inventory it is possible to assess, with some assumptions and simplifications, which

160   among the mapped landslides are able to dam their river section. Each landslide that is not already laying in the

161   valley floor with a volume bigger than V' and V" are identified as potentially prone to block the river in the future

162   in that point. Then, a "Map of Damming Susceptibility" for reactivation of existing landslides can be generated.

163   The likelihood prediction for new landslides, with volume bigger than V_l' and V_l'', is a much more difficult task

164   as the volume is a complex value to be estimated (Catani et al., 2016). The exceeding probability of landslide

165   volume used by Tacconi Stefanelli et al. (2020) was reached thanks to the knowledge of the alpha exponent of the

166   statistical frequency distribution of the landslide volumes in the whole study area. To achieve this, a database of

167   landslides with a very high number of events (tens or even hundreds of thousands) should be available (Catani et

168   al., 2016), which in our study area unfortunately is not. To have an assessment of the damming susceptibility for

169   neo-formed landslides the two volume threshold values, evaluated for all the river networks, can be used as well.

170   After estimating the river width of every river stretches, the V_l' and V_l'' values of each of them can be computed

171   through the corresponding two equations. In this way there will be two reference values to be able to assess whether

172   the volume of a new landslide can potentially obstruct an affected river stretch.

173   The input data needed for the procedure are a Digital Elevation Model, a vector layer of the river network, and an

174   updated landslide inventory. The data quality and resolution such as the landslides inventory completeness, the

175   river network reliability and the DEM's pixel size heavily affect the quality of the result (Tacconi Stefanelli et al.,

176   2020). Thus, it was decided to use the DEM with the higher resolution freely available from the NASA's SRTM

177   project (Far and Kobrick, 2000) with a 1 arc-second, or about 30 meters of resolution. The river network came

178   from Coccia et al., (2023). The latter input data is a database of 8910 landslides, that is a compilation of several

179   different inventories collected through decades of field surveys, studies and remote sensing analysis in the study

180   area, shown in Figure 3.

181   Hereafter the detail of each inventory:

182   •   The "Rockslides and Rock Avalanches of Central Asia" (Strom and Abdrakhmatov, 2018): an inventory

183   including more than 1000 of very big (>=1 Mm^3) rockslides and rock avalanches, covering central Asian countries

184   (excluding Turkmenistan and Altai) and also Chinese Tien Shan and Pamir, and Afghan Badakhshan. Collected

185   in decades of field survey and analysis of aerial/satellite imaging, it includes also information on morphometric

186   parameters (runout, area), dammed lakes, head-scarps, and quantitative characteristics (such as area, volume) for

187   about 600 cases.

188   •   The "Tien Shan landslide inventory" (Havenith et al., 2015a): is the biggest database in the study area.

189   Assembled through field work, remote sensing and geophysical data interpretation, it includes the elements of the

190   previous inventory alongside other smaller landslides in soft sediments (Havenith et al. 2006a; Schlögel et al.,

191   2011) for a total of 3,462 landslides polygons, including information on landslide length and area.

192   •   The "Multi-temporal landslide inventory for a study area in Southern Kyrgyz Republic derived from

193   RapidEye satellite time series data (2009 – 2013)" (Behling et al., 2014; 2016; 2020), includes 1,582 landslide

194   polygons mapped from multi-sensor optical satellite time series data (from 1986 to 2013) over an area of 2,500

195   km^2 in the Fergana valley rim in southern Kyrgyz Republic, and include information on landslide activity (area

196   and year of trigger).

197   •   The "Tajikistan landslide database" produced by the Institute of Water Problems, Hydropower,

198   Engineering and Ecology of Tajikistan (IWPHE), with 2,710 landslide polygons and 114 landslide-prone areas,

199   including information on landslides length and area.

200   •   The Institute of Seismology of the Academy of Science of Uzbekistan (ISASUZ) provided an inventory

201   which covers the Tashkent province composed by a point inventory (Nyazov R.A. 2020) and a polygon inventory

202   (345 landslide) digitized from the maps in Juliev et al., 2017.
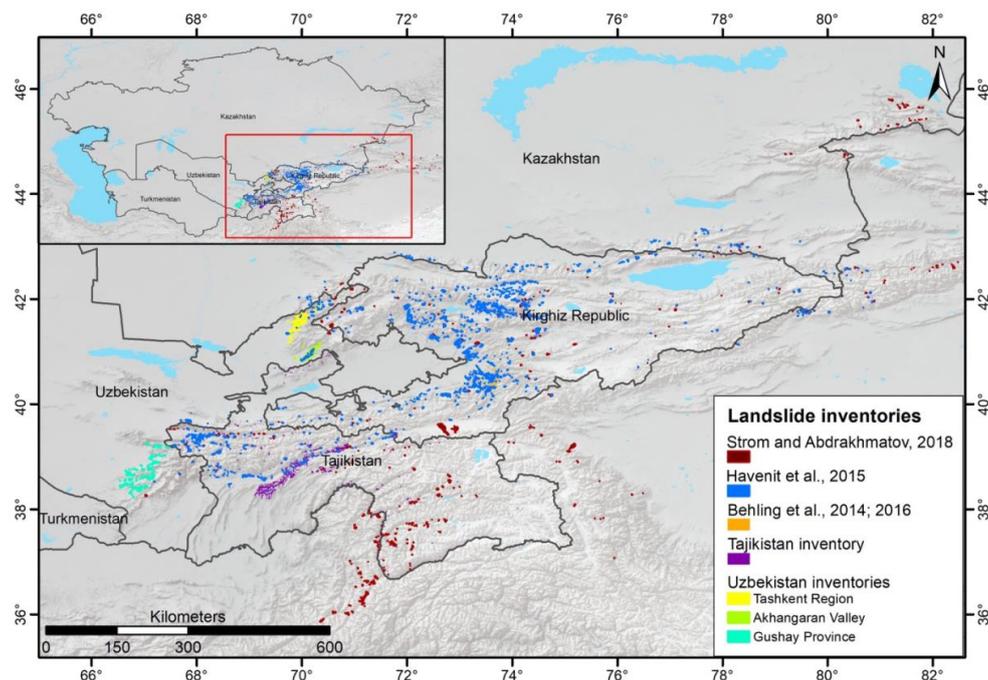
Figure 3. Map of the landslide inventories in the study area. Lake's polygons from Esri, Garmin International, Inc.; basemap from Esri, USGS, NOAA.

The methodology adopted to obtain the maps of damming susceptibility, derived from Tacconi Stefanelli et al. (2020), is summarized in the following main steps displayed in Figure 4. According to the literature (Swanson et al., 1986; Fan et al. 2014, 2020, 2021; Tacconi Stefanelli et al., 2015, 2018), river obstructions occur in most of the time within hilly or mountainous areas and specially along steep slopes. Therefore, considering the extension of the study area, in order to reduce the time of elaboration and improve the visualization of the results, in step I of Figure 4 a series of unnecessary data were removed from the calculations during some preliminary operations. For this reason, river that flaw in flat areas (with less than 4° slopes) were not considered in the elaborations, since their damming probability is certainly very low, and the potential impounded lake should have a negligible volume. Additionally, to have maps easier to manage and display, the river network was split in 5 km long river stretches consecutive to each other.
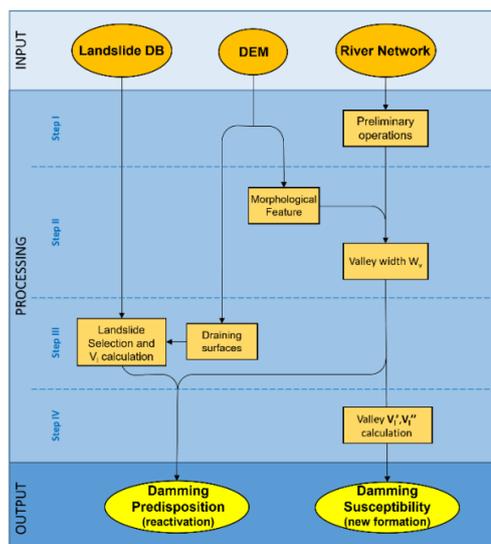
Figure 4. Flow chart of the main steps of the mapping methodology.

In applied geomorphology and natural science studies the analysis and characterization of the landscape has evolved during the last decades with the increasing accessibility of remote sensing data and the development of different algorithms able to automatically extract morphological features and landform information even at broad scales (Drăguţ and Dornik 2016; Maxwell and Shobe 2022; Righini and Surian 2018; Wang et al. 2010).

As already mentioned, the clear definition of the width of a river can be subjective and its measurement difficult to repeat especially if performed by different operators. In step II of Figure 4, an objective automatic method to extract morphometrical parameters have been chosen also for this reason. Wood (2009) implemented the "*LandSerf*" software (already incorporated in SAGA GIS or QGIS software), designed to automatically classify landforms from DEMs. Similarly for pattern detection and texture analysis within image processing, the software extracts land-surface parameters (e.g., slope, aspect, and curvature) from DEMs through a multi-scale approach. During these processing, the algorithm performs a classification of the landscape, grouping the landforms with homogeneous morphometric characteristics (pits, channels, peaks, ridges, passes, and planes) as shown in Figure 5. Thanks to this algorithm of morphological forms analysis proposed by Wood (2009), the polygons representing the morphological unit of the river valley can be automatically defined objectively even in a large area and extracted.

233
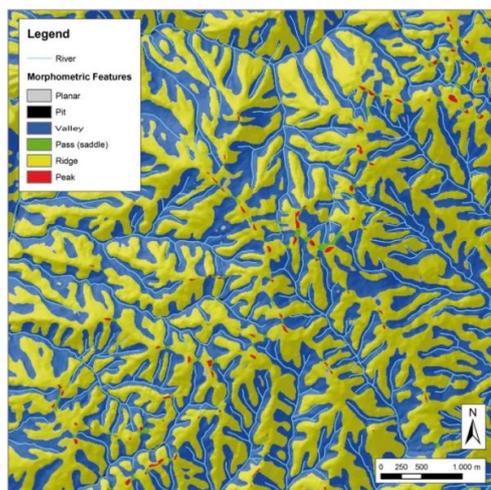
Figure 5. Classification of the landscape into morphological classes according to Wood (2009) (modified from Tacconi Stefanelli et al., 2020).

The effectiveness of distinguishing different morphological landforms of this automatic tool is greater in mountainous regions characterized by significant differences in elevation, compared to flat areas where distinctions between landforms are less evident. The accuracy of the output is directly correlated with the resolution of the DEM, which should ideally be about a few meters. Coarser resolutions result in landslide volumes with a corresponding level of uncertainty.

The following phase is to provide to each river stretch a value of a valley width, W_v. A series of 1 km long lines (hereafter "transects") are generated, perpendicular to the stretches of the river network, outdistanced by 500 meters apart from each other. The created river valley polygons are used to "cut" the transects and then to measure the distance between the two river valley borders through the length of the cut transects.

Next, the valley widths (W_v) for each segment of the river are determined by assigning them an average value based on N perpendicular transects, excluding the extreme values (maximum and minimum, respectively W_{max} and W_{min}), as in the fallowing equation:

$$W_v = (\sum_{i=1}^{n} W_i - W_{min} - W_{max}) \frac{1}{n-2} \qquad (4)$$

By utilizing an updated database of landslide polygons, in the step III of Figure 4 it is possible to determine if a reactivated landslide is big enough to cause a complete river blockage thanks to the comparison with the boundary volumes of V_l' (below which a landslide cannot completely block the river) and V_l'' (above which the river valley is dammed for sure). A reactivated landslide should follow a downhill path akin to the flow of surface water. Within each slope, the drainage directions can be easily determined along the river network using a GIS software. Each mass movement can then be linked to the corresponding river stretch it would reach if reactivated based on their corresponding draining surfaces.

Natural Hazards
and Earth System
Sciences
Discussions

256 Since the information provided by the available inventories in the study area are not homogeneous and comparable,

257 for the computation of the landslide volume were chose to use the areas of the landslide polygons, since it is the

258 most common data. An experimental statistical relationship between areas and volumes was applied:

259 $$V_l = \varepsilon \cdot A_l^{\alpha} \qquad (5)$$

260 where V_l and A_l are respectively the volume and the area of a landslide, ε and α are respectively the constant and

261 the exponent of the power law describing the landslides volumes frequency distribution. Various experimental

262 relations of ε and α have been employed for landslide volume calculations by researchers located in different

263 countries. After an evaluation of these relations in the study area, the parameter proposed by Guzzetti et al. (2009)

264 have been selected because of the number of the studied cases (667) and the magnitude range of the landslides

265 area investigated (from 10^1 to 10^9 m^2). The landslide volume computed using this procedure is based on some

266 approximations, since they use geometric simplifications, but it does still reflect the magnitude of the process. The

267 result of the computation in Figure 6 shows an almost bimodal distribution, in which most landslides (83%) have

268 moderate volumes, lower than 10 million m^3 (with 63% lower than 1 million m^3), but 4% have value higher than

269 100 million m^3.

270 Then, Table 1 is used to assign to each landslide of the inventory a classification based on the comparison with the

271 boundary volumes V_l' and V_l'', with value of 2 if the calculated landslide volume, V_l, is bigger than V_l' (or V_l''),

272 of 0 if it is smaller. For more caution, the V_l values is increased by an arbitrary value of 20% ($V_l \cdot 1.2$) to avoid

273 any potential underestimation during volume estimation and even the possible increase of landslide size with the

274 reactivation due to the mechanism of material entrainment (Hungr & Evans, 2004). For each landslide, if the

275 computed boundary volume V_l' (or V_l'') is bigger than the estimated landslide volume V_l, but smaller than $V_l \cdot$

276 1.2, then a classification value of 1 is attributed.

277 The damming susceptibility of each mapped landslide is assigned by integrating the two comparative classification

278 values from the intensity matrix illustrated in Figure 7. The matrix establishes five qualitative classes on a scale

279 of severity for damming susceptibility, ranging from Very Low (dark green) to Low (light green), Moderate

280 (yellow), High (orange), and Very High (red). The combination of a high V_l'' value (1 or 2) and a lower V_l' value

281 (0 or 1) symbolized by gray squares is not possible according to their respective formulations.
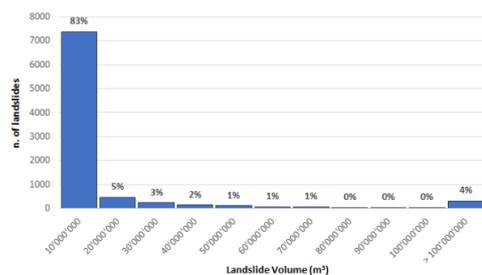
282

283 **Figure 6. Landslide volumes frequency distribution in the central Asia regions.**

284 **Table 1. Comparison table between landslide calculated volumes, V_l, with the boundary volume of Non-**

285 **formation and Formation, V_l' and V_l''(after Tacconi Stefanelli et al., 2020).**

	$V_1 > V_1'$ (V$_1$'')	$V_1 < V_1'$ (V$_1$'') < $V_1 * 1.2$	$V_1 < V_1'$ (V$_1$'')
Classification Value	2	1	0

286

287

Figure 7. Predisposition matrix used for the assignment of the damming predisposition intensity to the mapped landslides (after Tacconi Stefanelli et al., 2020).

Even if the proposed method is objective, it is certainly not free from uncertainties and errors. The 20% increase applied to mapped landslide volumes to reduce underestimation errors can in turn produce false positives for overestimation errors. While a false positive is preferable to a false negative (according to a principle of prudence), too many high-risk false positive cases "spread" an unreal risk throughout the area instead of concentrating it in sites of real risk. Therefore, it can be assumed that the landslide bodies which have previously reached the valley floor have already generated most of their effect on the river network (Strom, 2010) or have had no effect, spending their potential risk component. These landslides, also with a volume higher than V_1' and V_1'' and therefore classified with Very High dam predisposition, even if reactivated probably will not produce any further effect in the future. For these reasons, it was decided to downgrade the classification of those landslides that intersect the river network by reducing its position of the classification of damming predisposition by one class.

Using the W_v value for each river stretches estimated during the step III of Figure 4, in the last step (IV) the two boundary landslide volumes, namely "Non-formation volume" and "Formation volume" (V_1' and V_1''), can be estimated by applying the equations of the "Non-formation" (Eq. (2)) and "Formation" lines (Eq. (3)). These two values can be used both to classify the damming susceptibility of the river network (for new landslides) and of the landslides inventory (for their reactivation). For the first case, the computed volume values V_1' and V_1'' embody the required volumes of a new landslide to have a potential or certain (with 99% of confidence) obstruction for each river stretches.

12

Natural Hazards
and Earth System
Sciences
Discussions

Open Access

EGU

4   Results

The mapping methodology was applied to all the studied territories of the Central Asia region in order to analyze and evaluate the results. Two smaller basins, the upper Pskem river and the Fergana valley, were selected to verify the reliability at a catchment scale of the results obtained from a methodology applied on a national scale. The assessment of damming predisposition on the available landslide inventory on the Central Asia regions is shown in the map of Figure 8, while a closer detail is reported in Figure 10 showing the Kyrgyz Republic territory. The number of landslides (644 cases) classified with Very High damming predisposition from the whole inventory before the class reduction due to the river intersection was unjustifiably and unreasonably large posing excessive concern and risk perception. After the change, this number decreased by 75% up to 166 cases, a high number but more reasonable concerning such a large area. In the class distribution of the damming predisposition shown in Figure 9 the most frequent class is the Very Low, with 81% of the whole database, followed by the Low and High classes both with 6% and the remaining percentage divided among Moderate (5%) and Very High (2%).

This distribution is quite coherent with the landslide volumes frequency distribution since it is reasonable to associate landslides with very low volume (83%, shown in Figure 6) with those classified with very low susceptibility (81%, Figure 9). The landslides classified with the higher values of susceptibility (Moderate, High, and Very High with a total of 13%) instead do not only include landslides with higher volumes (more than 100 million m^3 representing 4% of the total), meaning that also even smaller landslides can potentially block narrow river stretches in these regions.
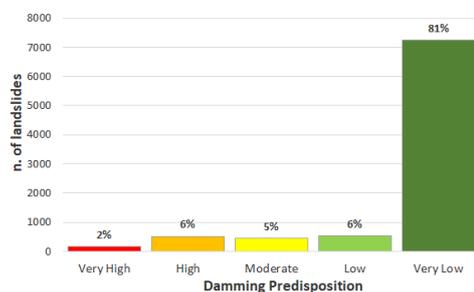
325
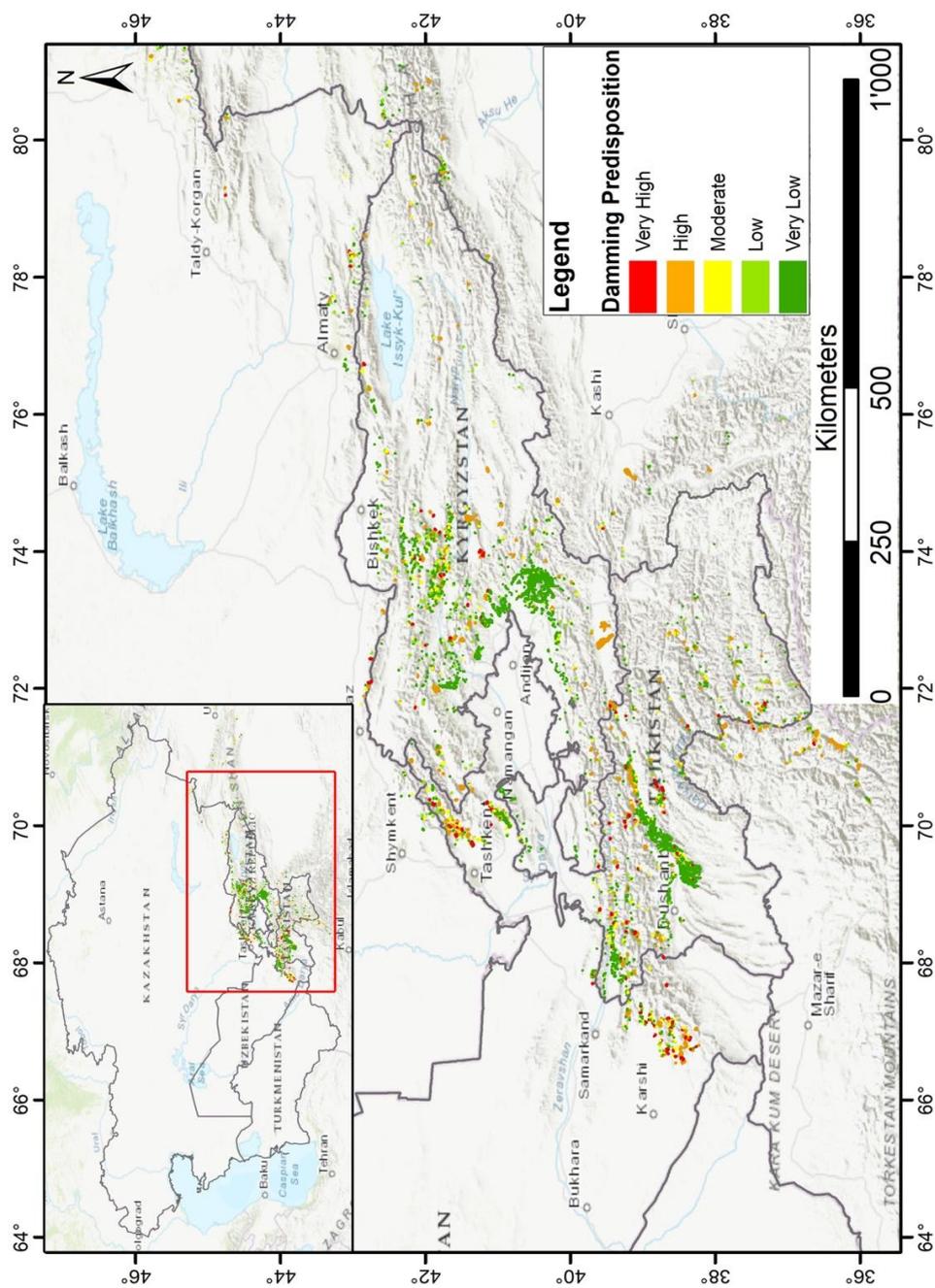
Figure 8. Map of Central Asia Landslide Damming Susceptibility. Basemap source: Esri, HERE, Garmin

Intermap, increment P Corp, GEBCO, USGS, FAO, NPS, NRCAN, GeoBase, IGN, Kadaster NL, Ordnance
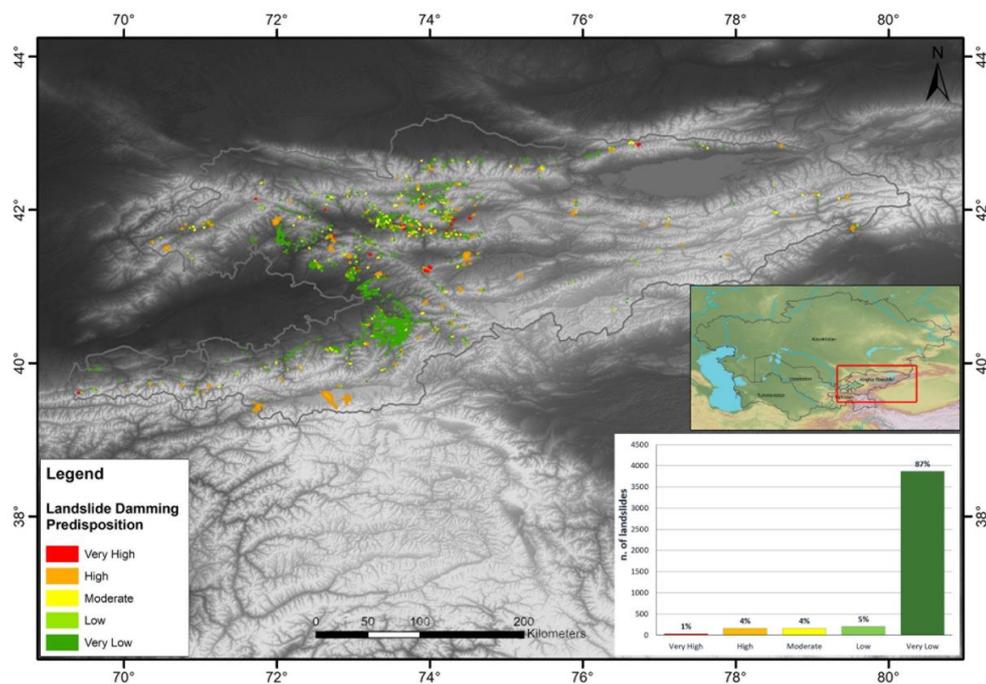
328   Survey, Esri Japan, METI, Esri China (Honk Kong), © OpenStreetMap contributors, and the GIS User

329   Community.

330

331

332   **Figure 9. Classes distribution of the damming predisposition for landslides reactivation.**

333

334   **Figure 10. Map of Damming Predisposition by landslides reactivation in Kyrgyz Republic territory.**

335   Topographic base from NASA's SRTM project (Far and Kobrick, 2000).

336   Concerning the damming susceptibility caused by new landslides along all the river network in the study area, two

337   different maps of the river networks have been produced using the Non-formation and Formation volumes values.

338   Although counterintuitive at first glance, these maps provide complementary information. The former provides

339   the volumes of landslides that surely create an obstruction, while the latter the volumes below which it definitely

15

340 does not form. According to the preliminary steps of the described methodology, in the river stretches running in

341 flat areas (slope degree less than 4° representing the 88.4% of the entire river network) the analysis has been not

342 applied, due to the extreme unlikelihood that a complete obstruction will occur in such areas. The magnitude of

343 the damming susceptibility of the river networks has been classified in five classes and shown in Figure 11 and

344 Figure 14. The five volumes intervals describing damming susceptibility were decided according to general value

345 distribution of landslides volumes and an expert judgement. Since small landslides are more frequent than large

346 ones, as reported in Figure 6, the lower is the landslide volume required to realize an obstruction, the higher is the

347 magnitude. In the map of damming susceptibility related to the "Non formation", reported in Figure 11, the central

348 classes, Moderate and Low are the most frequent with 4.4% and 5.8% respectively, as reported in Figure 12. This

349 means that in most of the river stretches in the study area the minimum landslide volume able to potentially dam

350 the riverbed is between the limit values of the two classes, from 2,5 to 25 million m^3. The following most frequent

351 class is the Very Low with 0.8% and only a very small portion of the river stretches are classified as High and

352 Very High with just 0.4% and 0.2% with a required landslide volume less than 2.5 million m^3. An example of

353 close-up on the Tajikistan territory is reported in Figure 13.

354 Regarding the map of damming susceptibility related to Formation values, the map in Figure 14 shows slightly

355 different results. The most frequent classes are the two lower ones, Low and Very Low with 4.4% and 6%

356 respectively, as described in Figure 15. Only just the 0.3% and 0.4% fall in the classes Very High and High

357 damming susceptibility. A close-up on the Kyrgyz Republic is reported in Figure 16.

358 The results of the classification for the river networks of each state are shown in Figure 17 to Figure 21. The

359 landslides of Tajikistan, Kyrgyz Republic, Uzbekistan and Kazakhstan regions have been classified according to

360 damming predisposition (Figure 17-a., Figure 18-a., Figure 19-a. and Figure 20-a). In the Turkmenistan territory,

361 it was not possible to assess any damming predisposition by landslides reactivation since the absence of any

362 available landslide inventory. The results of Uzbekistan and Kazakhstan regions (Figure 19-a. and Figure 20-a.)

363 are a bit different from Kyrgyz Republic and Tajikistan regions due to the different availability of landslide

364 inventories and a different reliefs orographic structure and valleys morphology of the formers national territories.

365 As already mentioned, for a clearer comprehension of the damming susceptibility classification of the river

366 network at the national level, the river stretches flowing in lowlands have not been considered in the analysis.

367 Concerning the Damming Susceptibility of Non-Formation (Figure 17-b., Figure 18-b., Figure 19-b., Figure 20-b.

368 and Figure 21-a.), the most frequent are Low and Moderate classes, followed by Very Low class. Fortunately, only

369 very few river stretches have been classified as Very High and High. For the Damming Susceptibility of Formation

370 (Figure 17-c., Figure 18-c., Figure 19-c., Figure 20-c. and Figure 21-b.) most of the rivers fall into Very Low and

371 Low classes, followed by Moderate class. Also in this case, only very few river stretches have been classified as

372 Very High and High. The results of the Tajikistan territory are quite similar to the Kyrgyz Republic and Uzbekistan

373 with which it shares a similar orographic distribution and morphology of the territory. Turkmenistan and

374 Kazakhstan show a slightly different distribution with higher percentage on Moderate class in the Damming

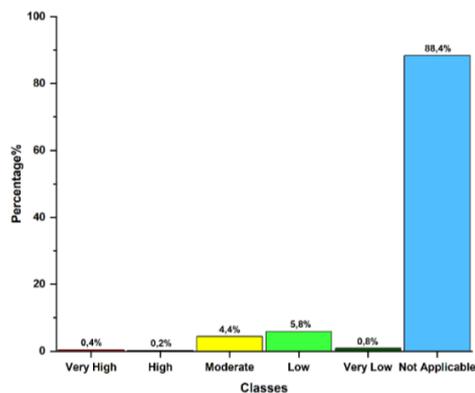375 Susceptibility of Non-Formation and Low class in the damming susceptibility of Formation.
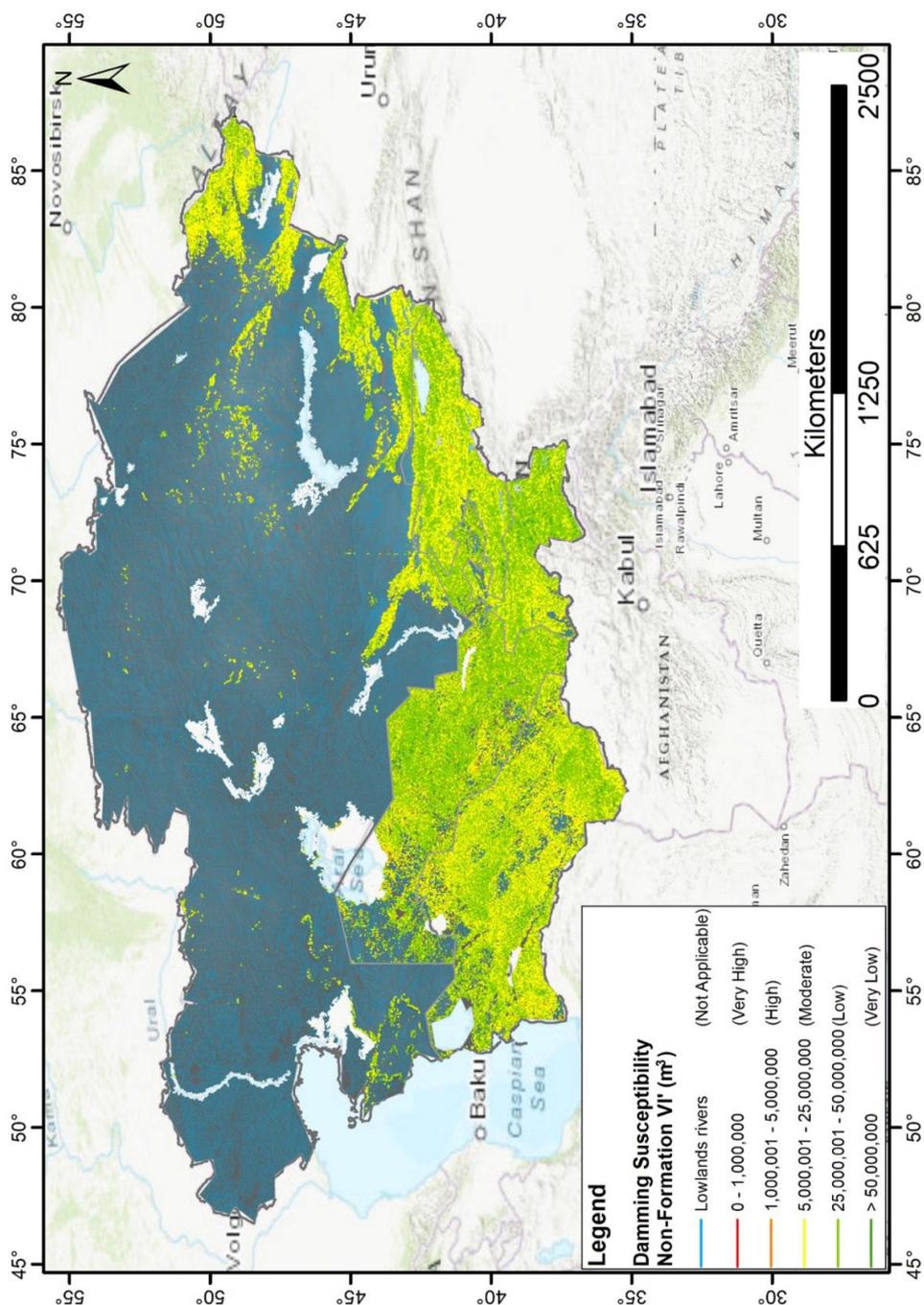
Figure 11. Damming susceptibility map of non-formation of river stretches by new landslides in the region. River network database from Coccia et al., (in prep.). Basemap source: Esri, HERE, Garmin Intermap,
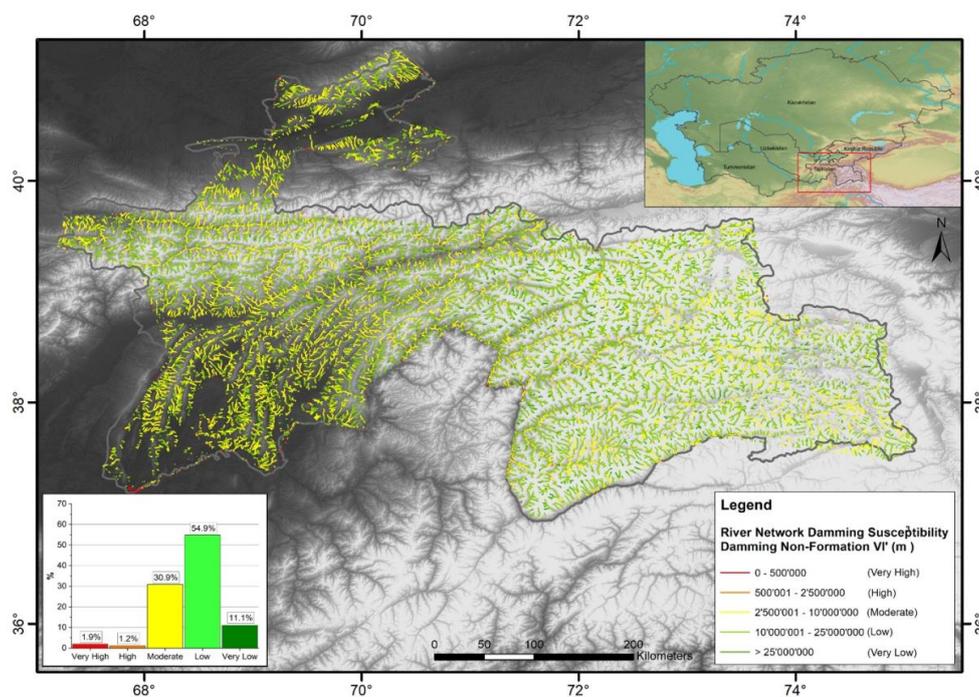
379 increment P Corp, GEBCO, USGS, FAO, NPS, NRCAN, GeoBase, IGN, Kadaster NL, Ordnance Survey, Esri

380 Japan, METI, Esri China (Honk Kong), © OpenStreetMap contributors, and the GIS User Community.
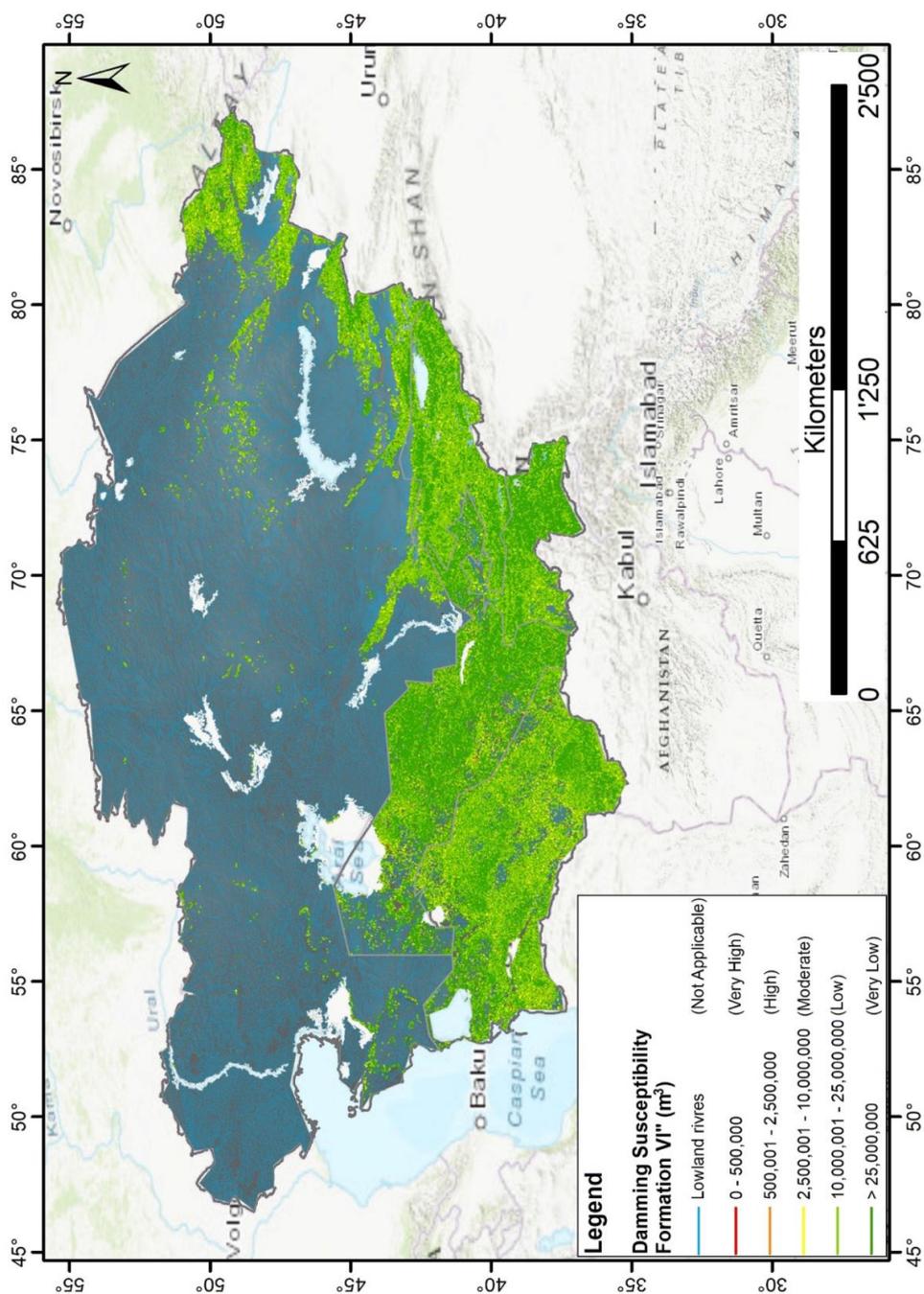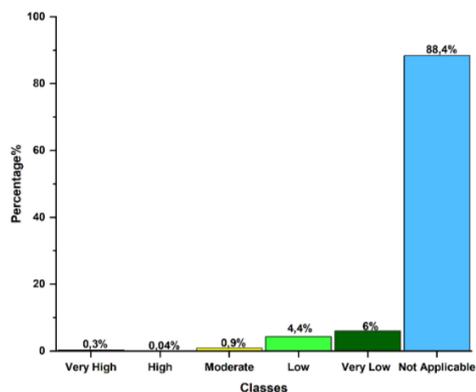

381

382 **Figure 12. Distribution of the damming susceptibility in the study area by new landslides related to Non**

383 **formation boundary values.**

384

385 **Figure 13. Damming Susceptibility Map of non-formation of river stretches by new landslides in**

386 **Tajikistan.** River network database from Coccia et al., (in prep.). Topographic base from NASA's SRTM

387 project (Far and Kobrick, 2000).

Figure 14. Damming Susceptibility Map of Formation of river stretches by new landslides in the region.

River network database from Coccia et al., (in prep.). Basemap source: Esri, HERE, Garmin Intermap, increment

391 P Corp, GEBCO, USGS, FAO, NPS, NRCAN, GeoBase, IGN, Kadaster NL, Ordnance Survey, Esri Japan,

392 METI, Esri China (Honk Kong), © OpenStreetMap contributors, and the GIS User Community.

393

394 **Figure 15. Distribution of the Damming Susceptibility in the study area by new landslides related to**

395 **Formation boundary values.**
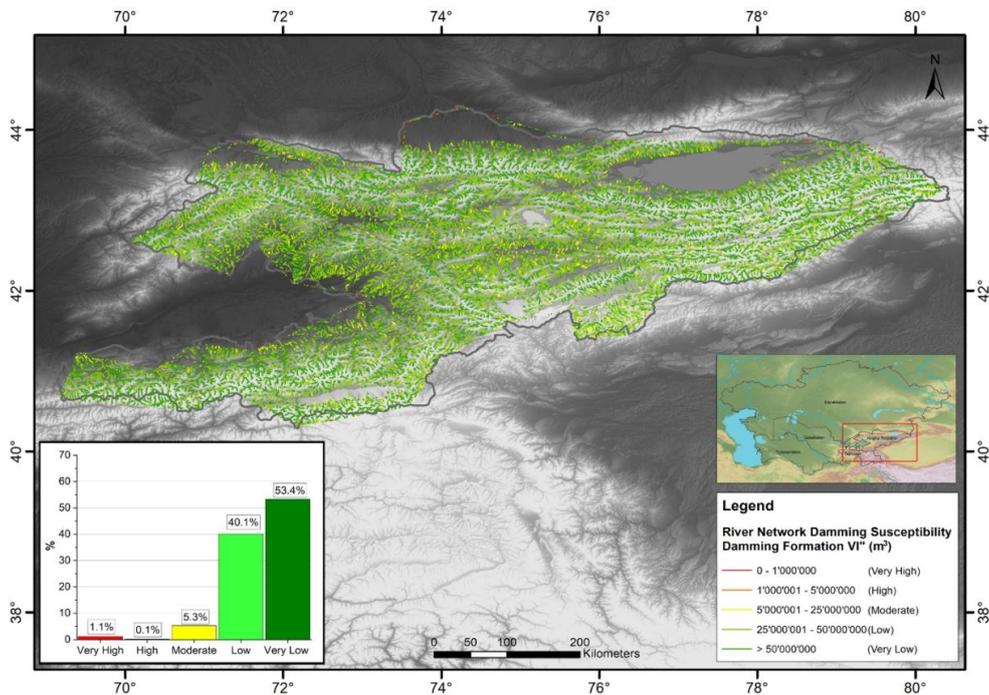
396

397 **Figure 16. Damming Susceptibility Map of formation of river stretches by new landslides in the Kyrgyz**

398 **Republic territory.** River network database from Coccia et al., (in prep.). Topographic base from NASA's

399 SRTM project (Far and Kobrick, 2000).

Natural Hazards
and Earth System
Sciences
Discussions
Open Access
EGU

400
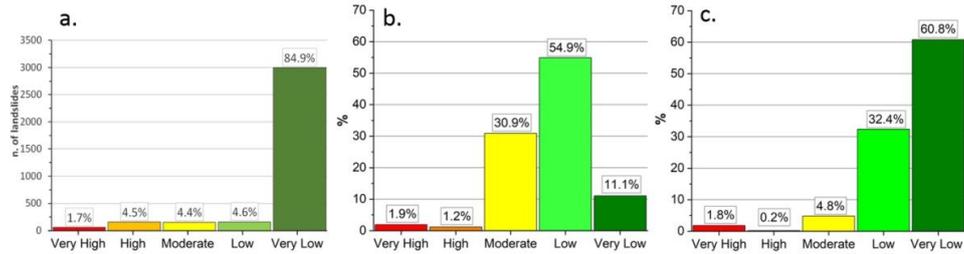
401 **Figure 17. Classes distribution in Tajikistan of the Damming Predisposition for landslides reactivation**

402 **(a.), Damming Susceptibility of Non-Formation (b.) and of Formation (c.) for new landslides.**
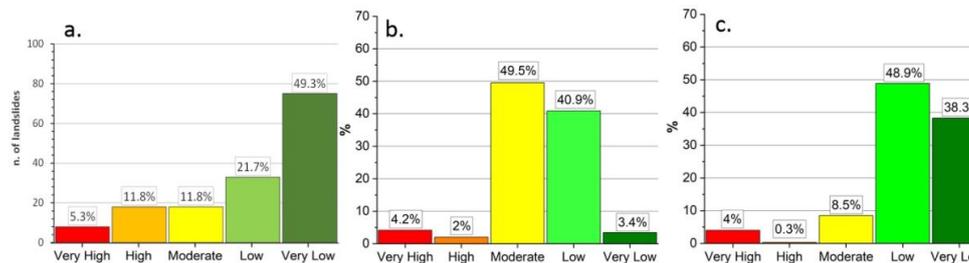
403
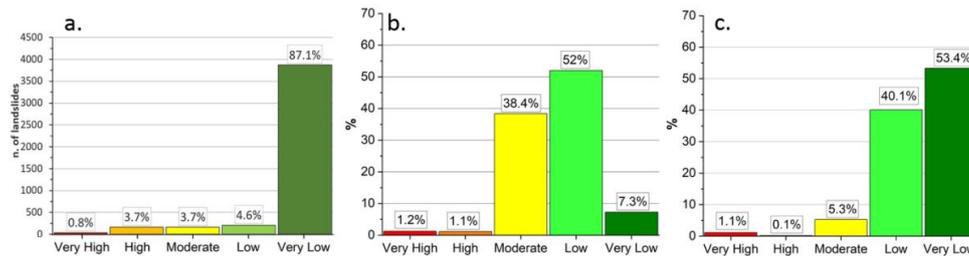
404 **Figure 18. Classes distribution in the Kyrgyz Republic of the Damming Predisposition for landslides**

405 **reactivation (a.), Damming Susceptibility of Non-Formation (b.) and of Formation (c.) for new landslides.**

406
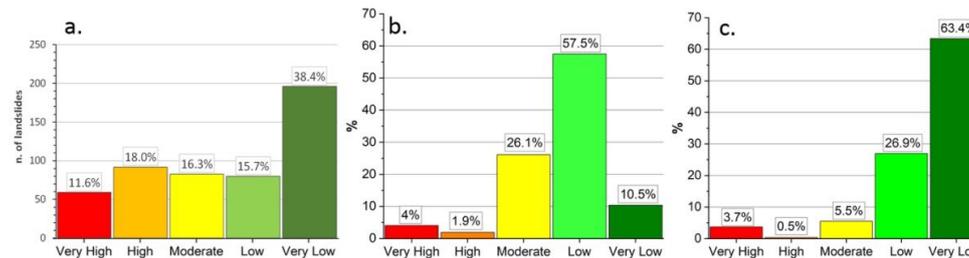
407 **Figure 19. Classes distribution in Uzbekistan of the Damming Predisposition for landslides reactivation**

408 **(a.), Damming Susceptibility of Non-Formation (b.) and of Formation (c.) for new landslides.**

409

Figure 20. Classes distribution in Kazakhstan of the Damming Predisposition for landslides reactivation (a.), Damming Susceptibility of Non-Formation (b.) and of Formation (c.) for new landslides.
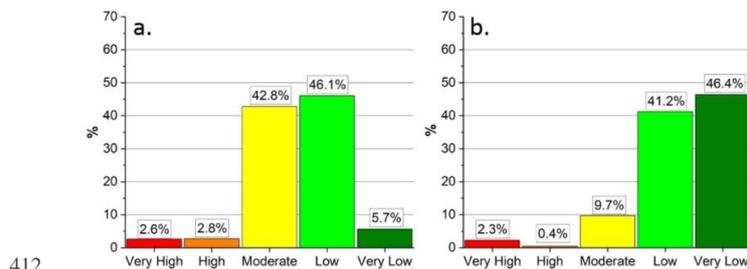
Figure 21. Classes distribution in Turkmenistan of the Damming Susceptibility of Non-Formation (a.) and of Formation (b.) for new landslides.

4.1   Upper Pskem river valley (Uzbekistan)

The Pskem river, locate in the Tashkent region of Uzbekistan, is a right-hand tributary of the Chirchik River that is the feeder of the Syr Darya river basin (in the Western Tien-Shan). The river originates from the confluence of the Maidantal and Oygaing rivers and is one of the main tributaries of the Charvak Lake (Semakova et al., 2016). This artificial lake is central for the local economy for its functions as reserve for fishing and water, as well as a source of hydroelectric energy and because of that various villages arise around it and downstream. The formation of a natural obstruction and an upstream impoundment in the Pskem basin could be a serious threat due to the possible instability of the earth dam and for the possible catastrophic cascade effects that its collapse could have downstream on the artificial basins and their 168 meters high earthfill dam.

With a careful observation of the map of Damming Predisposition by landslides reactivation in the lower Pskem basin in an area of 443 km^2 (Figure 22), some of the 53 mapped landslides should be subjected to further study. Among all, most landslides were classified with a Very Low and Low predisposition value, respectively 21 and 11 cases (39.6% and 20.8%), and only 4 landslides with a Very High value (7.5%), 10 with High (18.9%) and 7 with Moderate (13.2%). Landslides named A, B, C, D and E in Figure 22, if reactivated will potentially cause an obstruction of the main river section of the Pskem, being classified the first three and the latest two respectively with High and Very High damming predisposition. As shown in Table 2, the volumes of all these landslides are way bigger than the boundary volume of Non-Formation and Formation from Figure 23 and Figure 24. It is important to notice that the landslides A, B and C are laid down in the valley floor, meaning that in the past they had probably already dammed the river in that point, and the classification of their damming predisposition have been reduced by one, from Very High to High. Due to the considerable volumes of the landslides in the basin and the presence of landslides that have probably already blocked the river in the past, this relatively small area is certainly worthy of attention.

Table 2. Landslides volumes and damming parameters W$_v$, V$_l$', V$_l$" of the landslides in Figure 20 computed using the described method.

Landslide	V_1 - Landslide volume (m^3)	W_v – River Width (m)	V_1' - Volume of Non-formation (m^3)	V_1'' - Volume of Formation (m^3)
A	200.000.000	300	2.600.000	16.200.000
B	12.000.000	235	1.500.000	10.000.000
C	34.000.000	318	3.000.000	18.200.000
D	73.000.000	513	10.100.000	47.400.000
E	61.000.000	575	13.500.000	60.000.000

439
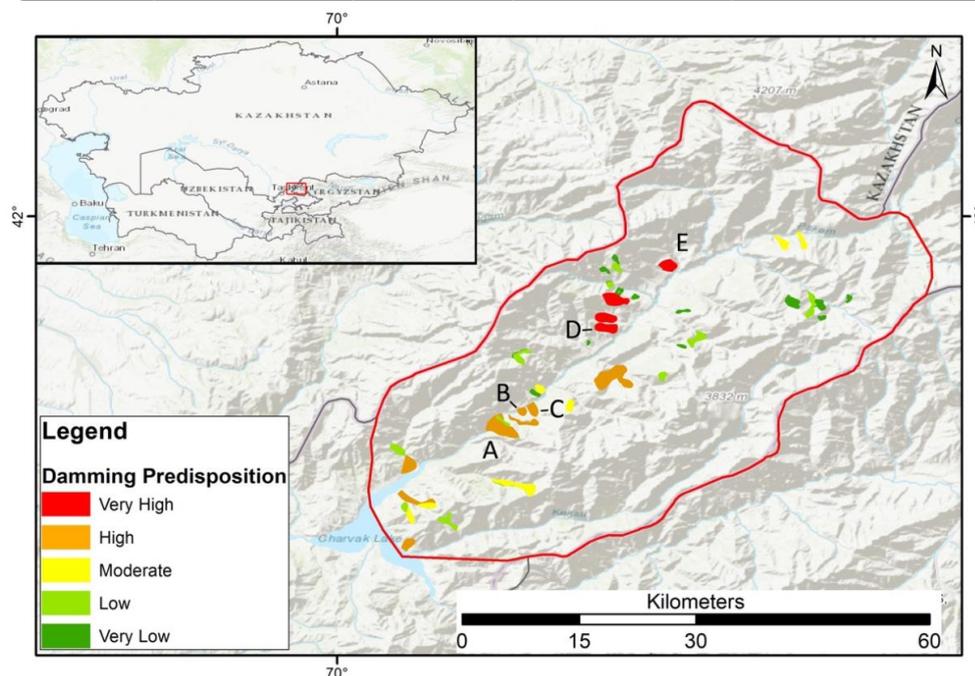
Figure 22. Map of Damming Predisposition by landslides reactivation in the lower Pskem basin. Basemap source: Esri, HERE, Garmin Intermap, increment P Corp, GEBCO, USGS, FAO, NPS, NRCAN, GeoBase, IGN, Kadaster NL, Ordnance Survey, Esri Japan, METI, Esri China (Honk Kong), © OpenStreetMap contributors, and the GIS User Community.

The obstruction of the Pskem river by one of these landslides would cause an upstream impoundment with a surface from 2 to 10 km^2 or more, depending on the dam position and height. The dam collapse could release a catastrophic flooding wave with destructive effects in the downstream areas. In the worst scenario, even the earthfill dam located few kilometers downstream could be seriously damaged with unpredictable effects. Since the reliability of this mapping method is strictly correlated to the quality of the input data, when the used DEM has a coarse resolution, in similar cases of possible risk to people's life it is always advisable to do a second "manual

23

450 check" even using some free satellite imaging services like Google Earth. In fact, when the DEM resolution is too

451 rough, the GIS tool used in this methodology to evaluate the extension of the riverbed morphologic unit can

452 produce inconsistent and incorrect results, causing improper damming susceptibility evaluations. The results of

453 the measurements on Google Earth orthophotos in Table 3 show that the difference between the river width values

454 calculated with the mapping method (W_v) and those measured on Google Earth (W_{vGE}) can in some cases be

455 substantial modifying the calculated boundary volumes V' and V'', although in this case they do not modify

456 drastically the final classification of the five landslides.

457 The river network of the upper Pskem valley have been also classified producing the maps of Damming

458 Susceptibility of Non-formation and Formation (Figure 23 and Figure 24 respectively). Concerning the Damming

459 Susceptibility Map of Non-formation (Figure 23), the most frequent are Low and Moderate classes with 65.1%

460 and 22.6% respectively, followed by Very Low class with 11.1%. Only just 1.3% have been classified as High and

461 0.0% as Very High. For the Damming Susceptibility Map of Formation (Figure 24) most of the rivers fall into

462 Very Low and Low classes with 69.8% and 27.7%, followed by Moderate class with 2.1%. Only 0.4% have been

463 classified as High and 0.0% as Very High.

464 **Table 3. Damming parameters W_{vGE}, $V_l'_{GE}$, $V_l''_{GE}$ of the landslides in Figure 22 computed with Google**

465 **Earth observation.**

| Landslide	W_{vGE} – River Width (m)	$V_l'_{GE}$ - Volume of non-formation (m³)	$V_l''_{GE}$ - Volume of Formation (m³)
A	415	6.000.000	31.000.000
B	310	2.800.000	17.300.000
C	260	1.800.000	12.100.000
D	530	11.000.000	50.000.000
E	450	7.300.000	36.500.000

466

467 The general damming susceptibility of the valley is low but a singular river stretch, marked by a black circle in

468 Figure 23 and Figure 24, classified with High susceptibility in both maps should be carefully evaluated. This river

469 part is clearly noticeable in the middle of the area along the main river path, a bit upstream from the landslides

470 named B and C. The high classification values mean that geographically in that point the valley width undergoes

471 a shrinkage and for this reason even a relatively small landslide generated from the surrounding slopes can create

472 an obstruction, therefore it would be worthy of a more detailed investigation.
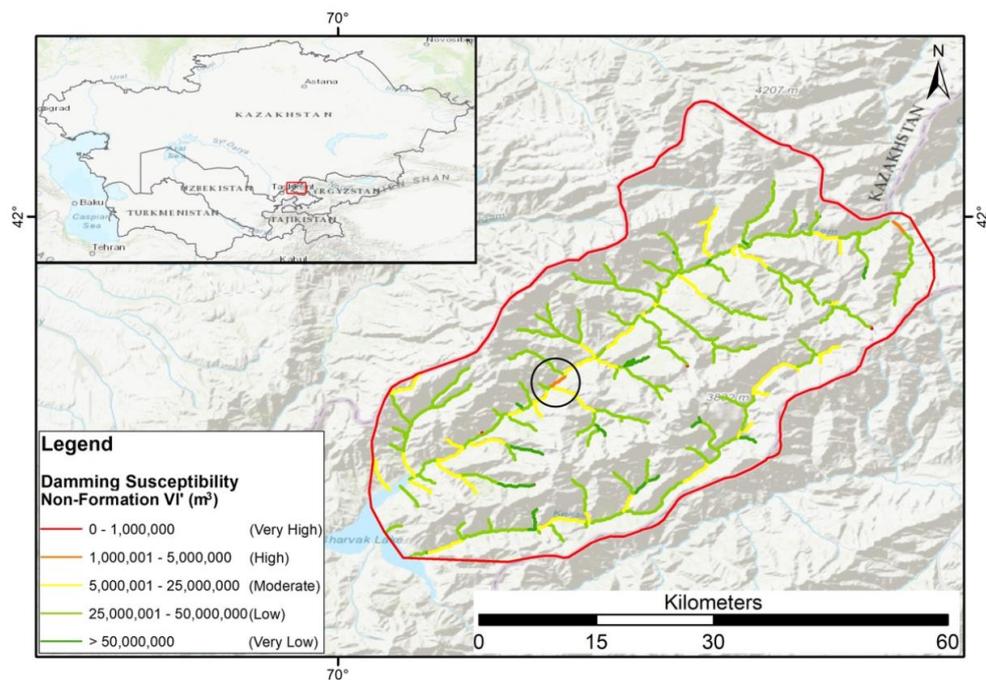
Figure 23. Damming Susceptibility Map of Non-formation of river stretches by new landslides in the lower Pskem basin. The black circle highlights a river stretch with unusually high values. River network database from Coccia et al., (in prep.). Basemap source: Esri, HERE, Garmin Intermap, increment P Corp, GEBCO, USGS, FAO, NPS, NRCAN, GeoBase, IGN, Kadaster NL, Ordnance Survey, Esri Japan, METI, Esri China (Honk Kong), © OpenStreetMap contributors, and the GIS User Community.
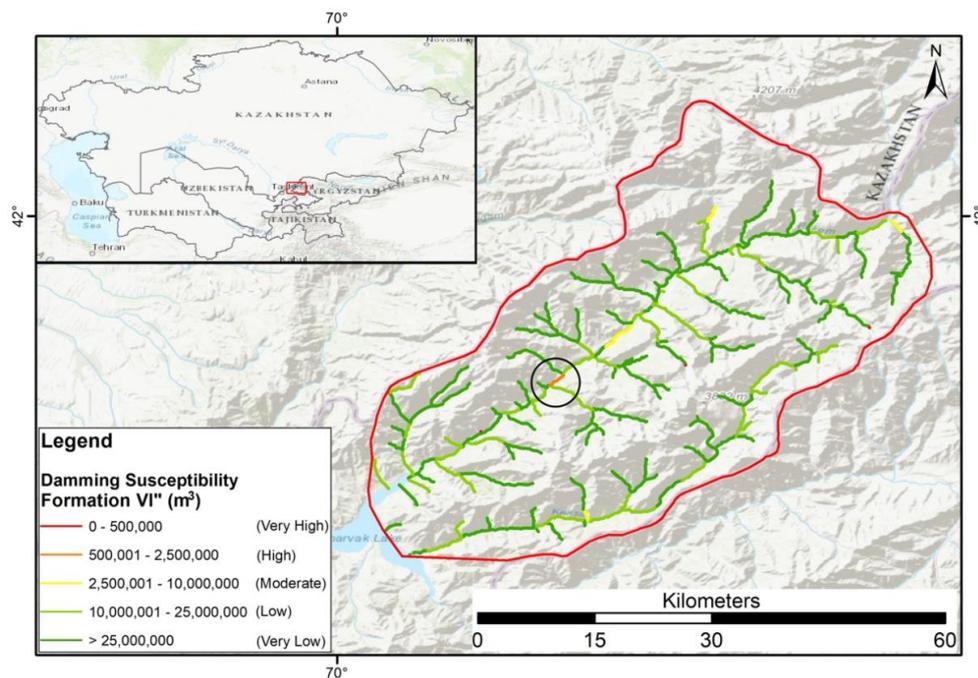
Figure 24. Damming Susceptibility Map of Formation of river stretches by new landslides in the lower Pskem basin. The black circle highlights a river stretch with unusually high values. River network database from Coccia et al., (in prep.). Basemap source: Esri, HERE, Garmin Intermap, increment P Corp, GEBCO, USGS, FAO, NPS, NRCAN, GeoBase, IGN, Kadaster NL, Ordnance Survey, Esri Japan, METI, Esri China (Honk Kong), © OpenStreetMap contributors, and the GIS User Community.

4.2 The Fergana valley mountainous rim (Tajikistan-Kyrgyz Republic-Uzbekistan)

The Fergana valley is one of the largest intermountain depressions in Central Asia located between Uzbekistan, Kyrgyz Republic, and Tajikistan. It hosts two main rivers, the Naryn and the Kara Darya, which join together to form the Syr Darya. In this populated area landslide activity is recurrent, causing every year damage to infrastructure and loss of human life, and triggered by complex interactions between multiple factors such as tectonic, geological, morphological and meteorological (Danneels et al., 2008; Schlöegel et al., 2011; Piroton et al., 2020). The mapping methodology have been applied also to the Fergana valley and a total of 3370 landslides, coming from various data sources, have been classified as shown in Figure 25. Comparably to the classification result of the entire inventory (Figure 8) most of the cases (94%) have a Very Low damming predisposition, followed by Low and Moderate (with 2.5% and 1.8% respectively) as reported in Table 4. Just very few landslides fall into High and Very High classes (with 1.4% and 0.3% respectively). For the classification of the river network of the Fergana valley, the maps of Damming Susceptibility of Non-formation and Formation have been produced (Figure 26 and Figure 27 respectively). As a method with a multi-scale approach, in such large areas, this damming

26

499 susceptibility method is suitable to provide territorial planning suggestions rather than indications on single

500 interventions at local scale. The overall damming predisposition of the Fergana valley is quite low, considering

501 the presence of 3370 mapped landslides in total, even if there are few landslides (10) classified with Very High

502 damming predisposition which should be studied with more attention through localized analysis of damming

503 susceptibility to ensure that downstream areas are not at risk and therefore require a specific monitoring.

504 Table 4 have been reported the distribution of the percentages of the damming susceptibility classes of those river

505 stretches that are not running in flat areas, since these lowland rivers represent 53.6% of the total. Concerning the

506 Damming Susceptibility Map of non-formation of the remaining river stretches (Figure 26), the most frequent are

507 Low and Moderate classes with 53.4% and 36.2% respectively, followed by Very Low class with 7.0%. Only just

508 2.1% and 1.3% have been classified as Very High and High. For the Damming Susceptibility Map of Formation

509 (Figure 27) most of the rivers fall into Very Low and Low classes with 54.5% and 38.1%, followed by Moderate

510 class with 5.2%. Only 1.9% and 0.2% have been classified as Very High and High respectively.

511 **Table 4. Distribution of Damming Susceptibility classes on existing landslides (Figure 25) and on the river**

512 **stretches for non-formation (Figure 26) and Formation of new landslides (Figure 27).**
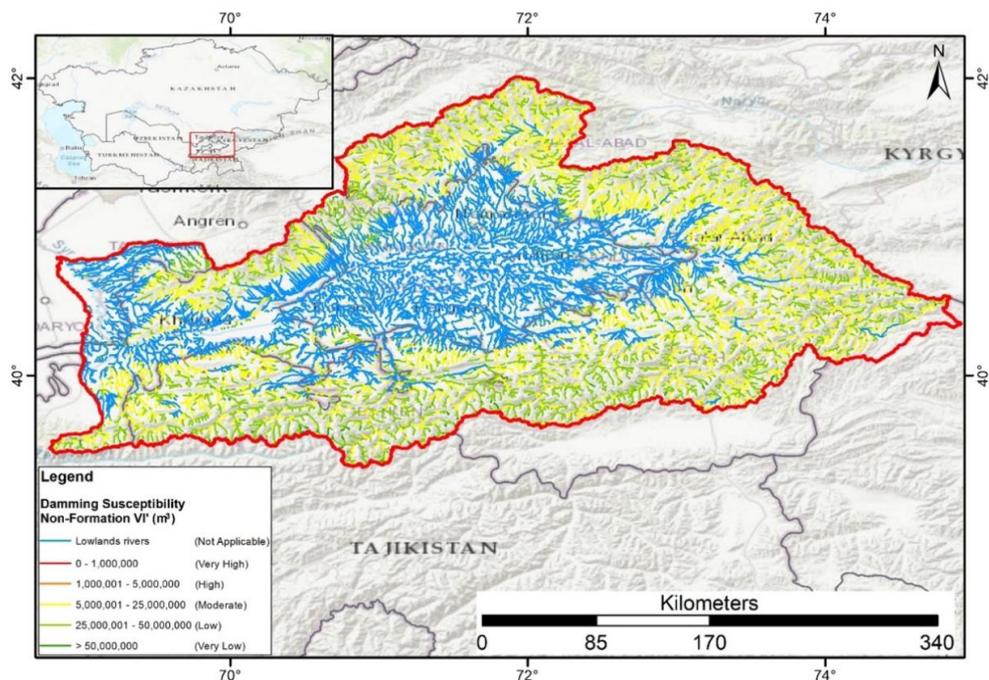
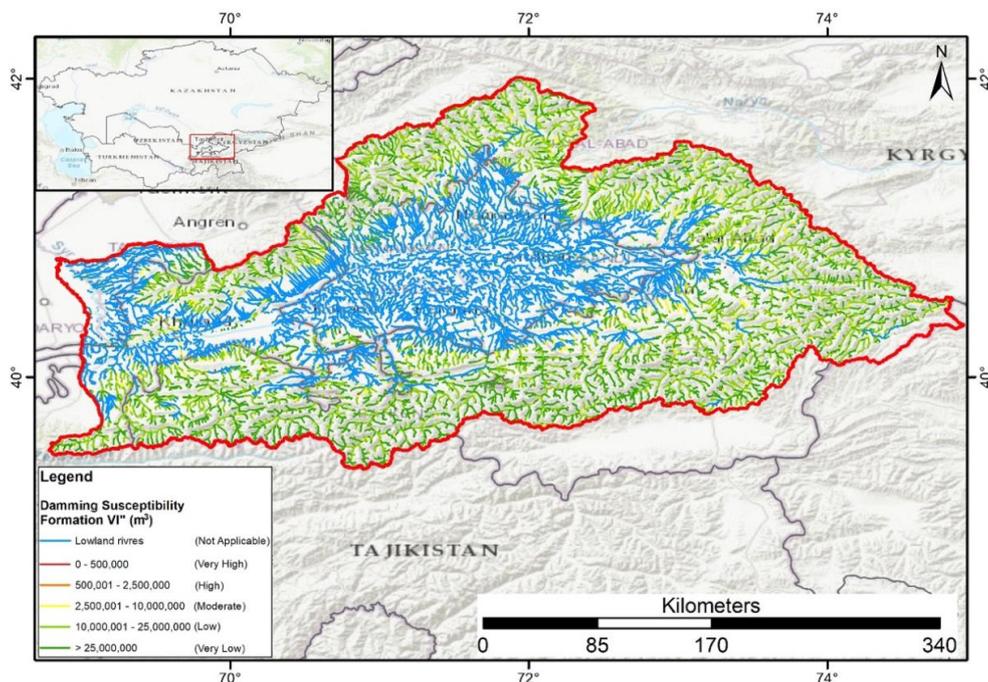| Damming Susceptibility	Landslides		non-formation	Formation
	n.	%	%	%
Very High	10	0.3%	1.9	1.7
High	48	1.4%	1.2	0.2
Moderate	61	1.8%	7.0	5.3
Low	83	2.5%	53.2	38.8
Very Low	3168	94.0%	6.7	54.0

513
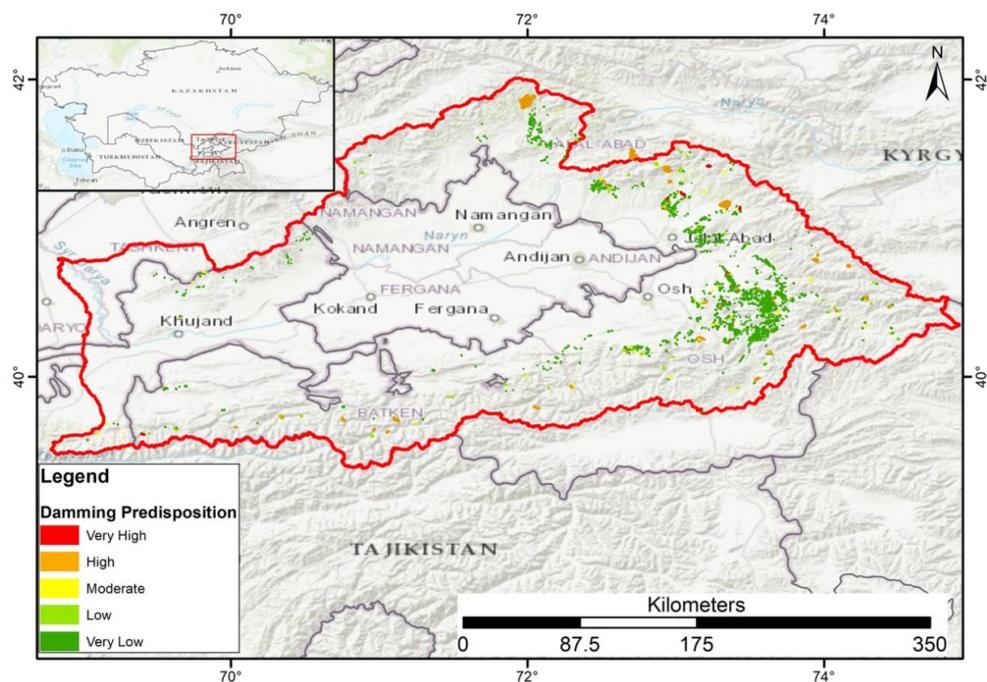
Figure 25. Map of Damming Predisposition by landslides reactivation in the Fergana valley. Basemap source: Esri, HERE, Garmin Intermap, increment P Corp, GEBCO, USGS, FAO, NPS, NRCAN, GeoBase, IGN, Kadaster NL, Ordnance Survey, Esri Japan, METI, Esri China (Honk Kong), © OpenStreetMap contributors, and the GIS User Community.

Natural Hazards
and Earth System
Sciences
Discussions

Open Access

EGU

519

Figure 26. Damming Susceptibility Map of Non-formation of river stretches by new landslides in the Fergana valley. River network database from Coccia et al., (in prep.). Basemap source: Esri, HERE, Garmin Intermap, increment P Corp, GEBCO, USGS, FAO, NPS, NRCAN, GeoBase, IGN, Kadaster NL, Ordnance Survey, Esri Japan, METI, Esri China (Honk Kong), © OpenStreetMap contributors, and the GIS User Community.

Figure 27. Damming Susceptibility Map of Formation of river stretches by new landslides in the Fergana valley. River network database from Coccia et al., (in prep.). Basemap source: Esri, HERE, Garmin Intermap, increment P Corp, GEBCO, USGS, FAO, NPS, NRCAN, GeoBase, IGN, Kadaster NL, Ordnance Survey, Esri Japan, METI, Esri China (Honk Kong), © OpenStreetMap contributors, and the GIS User Community.

5   Discussion

During the application of the damming mapping methodology, the main issues encountered was the extremely wide study area, the amount of data and the processing time required. The used mapping methodology based on the MOI equations (Eq.(1)), was originally designed to assess the damming susceptibility at basin/regional scale (Tacconi Stefanelli et al., 2016; 2020), where the morphological parameters essential for the correct application of the tool proposed by Wood (2009) must be correctly found to have an accurate river width required in the MOI equations (Eq.(1)). This time-consuming phase has been simplified in this research, according to the wide dimension of the study area, taking into account not the basins but the different states in the Central Asia region. Furthermore, the results quality is directly proportional to the resolution and quality of the input data, which on the other hand is inversely proportional to the processing time. In this regard, a further criticality of this process is the reliability on the landslides volumes assessment method, since a higher quality of landslides data (sliding geometry and depth) allows the application of a more accurate volume calculation and therefore a better final result.

543   Thus, even if the results are not always highly reliable at local scale, requiring many in-depth specific studies in

544   the areas identified with the higher predisposition, they can be undoubted useful in very large countries to adopt

545   risk reduction measures, for planning purposes and for land development management.

546   Considering the size of the area, in Figure 10 the number of landslides classified with Very High damming

547   predisposition (166 cases) is reasonable in absolute value, even if a bit high if compared with the total number of

548   landslides present in the inventory (8910 cases). Without a detailed study it is not possible to say how many of

549   these are false positives or not, however it is important to remember that this type of risk mapping methods gives

550   information on if and where, not when these events may occur.

551   The two maps of damming susceptibility (Figure 11 and Figure 14), while not providing probability values as done

552   by Tacconi Stefanelli et al. (2020), offer information (the volumes of landslides) that can be more easily spent and

553   interpreted even by operators who are not specifically expert, and for this reason have more practical utility.

554   Furthermore, the classification of the river stretches thus produced, not requiring the alpha parameter (linked to

555   the probability of landslide occurrence) as in the original method proposed by Tacconi Stefanelli et al. (2020), it

556   is much easier to obtain and for this reason it can be considered an improvement within a view of wider usability.

557   **6   Conclusions**

558   The price of a river obstruction, in terms of reconstruction and losses on both economic and lives, can be much

559   higher compared with the costs of a proper environmental planning and land-use management. Be able to define

560   the areas with higher risk could considerably lower the costs, allowing to focus the economic resources in effective

561   preventive interventions, planning and monitoring activities.

562   In this work a damming mapping methodology have been proposed and carried out on the Central Asia regions.

563   The used method, originally developed applying the Morphological Obstruction Index at basin scale, have been

564   modified to fit such a large study area and the available data. The improvement of the original method allows a

565   simpler use and the need for less data, more easily available, although the absence of a validation of the results

566   inevitably remains. The main aim of this study was to propose a practical tool to assess where the damming

567   susceptibility from reactivation of mapped landslides and formation of new landslides are higher at national scale.

568   This second result of the mapping damming susceptibility from new landslide can be particularly useful in area of

569   the world where there is a lack of diffuse assessment of landslide activity and incomplete landslide inventories.

570   *Code and data availability*. The landslide dam mapping susceptibility method was implemented by using the cited

571   landslide inventory maps, published by the following authors: Behling et al., 2014, 2016, 2020; Havenith et al.,

572   2015a; Strom and Abdrakhmatov, 2018. The SRTM DEM data are available from https://earthexplorer.usgs.gov/.

573   The river network and other landslide inventories were provided by the SFRAAR project partners: RED (Risk,

574   Engineering + Development – Pavia, Italy), OGS (National Institute of Oceanography and Experimental

575   Geophysics, Seismological Research Center, Trieste, Italy), IWPHE (Institute of Water problems, Hydropower,

576   Engineering and Ecology, Dushanbe, Republic of Tajikistan), ISASUZ (Institute of Seismology of the Academy

577   of Science of Uzbekistan, Tashkent, Uzbekistan), LLP (Institute of Seismology of the Science Committee of the

578   Republic of Kazakhstan, Almaty).

References

Abdrakhmatov, K.Y., Aldazhanov, S.A., Hager, B.H., Hamburger, M.W., Herring, T.A., Kalabaev, K.B., Makarov, P. Molnar, S.V. Panasyuk, M.T. Prilepin, R.E. Reilinger, I.S. Sadybakasov, B.J. Souter, Yu.A. Trapeznikov, V.Ye., and Tsurkov Zubovich, A.V.: Relatively recent construction of the Tien Shan inferred from GPS measurements of present-day crustal deformation rates. Nature, 384(6608), 450-45319, 1996.

Abdrakhmatov, K., Havenith, H.B., Delvaux, D., Jongmans, D., and Trefois, P.: Probabilistic PGA and Arias Intensity Maps of Kyrgyz Republic (Central Asia). J. Seismol. 7.2: 203-220, 2003.Akgun, A. A comparison of landslide susceptibility maps produced by logistic regression, multi-criteria decision, and likelihood ratio methods: A case study at İzmir, Turkey. Landslides 2012, 9, 93–106.

Bazzurro, P. et al.: Strengthening Financial Resilience and Accelerating Risk Reduction in Central Asia – the SFRARR project. The SFRARR probabilistic flood hazard assessment, in preparation, 2023.

615 Behling, R., Roessner, S., Kaufmann, H., and Kleinschmit, B.: Automated spatiotemporal landslide mapping over
616   large areas using rapideye time series data. Remote Sens. 6, 8026–8055, 2014.

617 Behling, R., Roessner, S., Golovko, D., and Kleinschmit, B.: Derivation of long-term spatiotemporal landslide
618   activity—A multi-sensor time series approach. Remote Sens. Environ. 186, 88–104, 2016.

619 Behling, R., and Roessner, S.: Multi-temporal landslide inventory for a study area in Southern Kyrgyz Republic
620   derived from RapidEye satellite time series data (2009 – 2013). V. 1.0. GFZ Data Services.
621   https://doi.org/10.5880/GFZ.1.4.2020.001, 2020.

622 Borgatti, L., and Soldati, M.: Landslides as a geomorphological proxy for climate change: a record from the
623   Dolomites (northern Italy), Geomorphology, 120(1–2), 56–64, 2010.

624 CAC DRMI: Risk assessment for Central Asia and Caucasus: desk study review, 2009.

625 Canuti. P., Casagli, N., Ermini, L., Fanti, R., and Farina, P.: Landslide activity as a geoindicator in Italy:
626   significance and new perspectives from remote sensing, Environ. Geol., 45(7), 907–919, 2004.

627 Casagli, N., and Ermini, L.: Geomorphic analysis of landslide dams in the Northern Apennine, Trans. Jpn.
628   Geomorphol. Union., 20(3), 219–249, 1999.

629 Catani, F., Tofani, V., and Lagomarsino, D.: Spatial patterns of landslide dimension: a tool for magnitude mapping,
630   Geomorphology 273, 361–373. https://doi.org/10.1016/j.geomorph.2016.08.032, 2016.

631 Chedia, O.K., and Lemzin, I.N.: Seismogenerating faults of the Chatkal depression. In: Seismotectonics and
632   seismicity of the Tien Shan. Frunze, Ilim, 18–28, 1980.

633 Coccia, G. et al.: The SFRARR probabilistic flood hazard assessment, NHESS, in preparation, 2023.

634 Costa, J.E., and Schuster, R.L.: Documented historical landslide dams from around the world. US Geol. Surv.
635   Open-File Report, 91(239), 1-486, 1991.

636 Crozier, M.J.: Deciphering the effect of climate change on landslide activity: a review, Geomorphology, 124(3),
637   260–267, 2010.

638 Dal Sasso, S.F., Sole, A., Pascale, S., Sdao, F., Bateman Pinzòn, A., and Medina, V.: Assessment methodology
639   for the prediction of landslide dam hazard, Nat. Hazards Earth Syst. Sci., 14 (3), 557–567,
640   http://dx.doi.org/10.5194/nhess-14-557-2014, 2014.

641 Danneels, G., Bourdeau, C., Torgoev, I., Havenith, H. B. Geophysical investigation and dynamic modelling of
642   unstable slopes: case-study of Kainama (Kyrgyzstan). Geophys. J. Int., 175(1), 17-34, 2008.

643 Delvaux, D., Abdrakhmatov, K.E., Lemzin, I.N., and Strom, A.L.: Landslides and surface breaks of the 1911 Ms
644   8.2 Kemin earthquake, Kyrgyzstan, Russian Geology and Geophysics, 2001, 42, 10, 1667-1677, 2001.

645 Dikau, R., and Schrott, L.: The temporal stability and activity of landslides in Europe with respect to climatic
646   change (TESLEC): main objectives and results, Geomorphology, 30(1–2), 1–12, 1999.

647 Drăguţ, L., and Dornik, A.: Land-surface segmentation as a method to create strata for spatial sampling and its
648   potential for digital soil mapping, Int. J. Geogr. Inf. Sci., 30(7), 1359-1376, 2016.

649 Fan, X., Rossiter, D.G., van Westen, C.J., Xu, Q., and Görüm, T.: Empirical prediction of coseismic landslide dam
650   formation, Earth. Surf. Proc. Land., 39(14), 1913–1926, 2014.

651 Fan, X., Dufresne, A., Subramanian, S.S., Strom, A., Hermanns, R., Tacconi Stefanelli, C., Hewitt, K., Yunus,
652   A.P., Dunning, S., Capra, L., Geertsema, M., Miller, B., Casagli, N., Jansen, J.D., and Xu, Q.: The formation
653   and impact of landslide dams – State of the art, Earth Sci. Rev., 203, 103116,
654   https://doi.org/10.1016/j.earscirev.2020.103116, 2020.

655 Fan, X., Dufresne, A., Whiteley, J., Yunus, A. P., Subramanian, S.S., Okeke, C. A., Pánek, T., Hermanns, R.,
656   Ming, P., Strom, A., Havenith, H.-B., Dunning, S., Wang, G., and Tacconi Stefanelli, C.: Recent
657   technological and methodological advances for the investigation of landslide dams, Earth-Sci. Rev., 218,
658   103646, https://doi.org/10.1016/j.earscirev.2021.103646, 2021.

659 Farr, T.G., and Kobrick, M.: Shuttle Radar Topography Mission produces a wealth of data. Eos Trans. AGU, 81,
660   583-583, 2000.

661 Golovko, D., Roessner, S., Behling, R., Wetzel, H. U., and Kleinschmidt, B.: Development of multi-temporal
662   landslide inventory information system for southern Kyrgyz Republic using GIS and satellite remote sensing,
663   PFG, 2015(2), 157–172, 2015.

664 Guzzetti, F., Ardizzone, F., Cardinali, M., Rossi, M., and Valigi, D.: Landslide volumes and landslide mobilization
665   rates in Umbria, central Italy, EPSL, 279, 222–229, 2009.

666 Havenith, H.B., Strom, A., Cacerez, F., and Pirard, E.: Analysis of landslide susceptibility in the Suusamyr region,
667   Tien Shan: statistical and geotechnical approach. Landslides 3, 39–50, 2006a.

668 Havenith, H.B., Torgoev, I., Meleshko, A., Alioshin, Y., Torgoev, A., and Danneels, G.: Landslides in the Mailuu-
669   Suu Valley, Kyrgyz Republic—hazards and impacts, Landslides, 3, 137–147, 2006b.

670 Havenith, H.B., Strom, A., Torgoev, I., Torgoev, A., Lamair, L., Ischuk, A., and Abdrakhmatov, K.: Tien Shan
671   geohazards database: Earthquakes and landslides, Geomorphology, 249, 16–31, 2015a.

672 Havenith, H.B., Torgoev, A., Schlögel, R., Braun, A., Torgoev, I., and Ischuk, A.: Tien Shan geohazards database:
673   Landslide susceptibility analysis, Geomorphology, 249, 32–43, 2015b.

674 Havenith, H.B., Umaraliev, R., Schlögel, R., Torgoev, I., Ruslan, U., Schlogel, R., and Torgoev, I.: Past and
675   Potential Future Socioeconomic Impacts of Environmental Hazards in Kyrgyz Republic. In Kyrgyz Republic:
676   Political, Economic and Social Issues; Olivier, A.P., Ed.; Nova Science Publishers, Inc.: Hauppauge, NY,
677   USA; pp. 63–113, 2017.

678 Hungr, O., and Evans, S.G.: Entrainment of debris in rock avalanches: an analysis of a long run-out mechanism,
679   Geol. Soc. Am. Bull., 116(9-10), 1240-1252, 2004.

Natural Hazards
and Earth System
Sciences
Discussions

680 Kalmetieva, Z.A., Mikolaichuk, A.V, Moldobekov, B.D., Meleshko, A. V, Janaev, M.M., and Zubovich, A.V.:
681   Atlas of earthquakes in Kyrgyz Republic. Central-Asian Institute for Applied Geosciences and United
682   Nations International Strategy for Disaster Reduction Secretariat Office in Central Asia, Bishkek, p 75, 2009.

683 Liao, H. M., Yang, X. G., Lu, G. D., Tao, J., and Zhou, J. W.: A geotechnical index for landslide dam stability
684   assessment,   Geomatics,   Natural   Hazards   and   Risk,   13(1),   854-876,
685   https://doi.org/10.1080/19475705.2022.2048906, 2022.

686 Maxwell, A.E., and Shobe, C.M.: Land-surface parameters for spatial predictive mapping and modeling, Earth-
687   Sci. Rev., 226, 103944, 2022.

688 Molnar, P., and Tapponnier, P.: Cenozoic Tectonics of Asia: Effects of a Continental Collision: Features of recent
689   continental tectonics in Asia can be interpreted as results of the India-Eurasia collision. science, 189(4201),
690   419-426, 1975.

691 Niyazov R.A.: Uzbekistan landslides. Uzbekistan landslide service. Technical report, 2020.

692 Petrov, M.A., Sabitov, T.Y., Tomashevskaya, I.G., Glazirin, G.E., Chernomorets, S.S., Savernyuk, E.A.,
693   Tutubalina O.V., Petrakov, D.A., Sokolov, L.S., Dokukin, M.D., Mountrakis, G., Ruiz-Villanueva, V., and
694   Stoffel, M.: Glacial lake inventory and lake outburst potential in Uzbekistan, Sci. Total Environ., 592, 228-
695   242, 2017.

696 Piroton, V., Schlögel, R., Barbier, C., and Havenith, H.B.: Monitoring the recent activity of landslides in the
697   Mailuu-suu valley (Kyrgyz Republic) using radar and optical remote sensing techniques. Geosciences, 10
698   (5), p. 164, 2020.

699 Popescu, M.E., and Sasahara, K.: Engineering Measures for Landslide Disaster Mitigation, in: Landslides –
700   Disaster Risk Reduction, edited by: Sassa, K., Canuti, P., Springer, Berlin, Heidelberg, 609-631,
701   https://doi.org/10.1007/978-3-540-69970-5_32, 2009.

702 Righini, M., and Surian, N.: Remote sensing as a tool for analysing channel dynamics and geomorphic effects of
703   floods, Flood monitoring through remote sensing, 27-59, 2018.

704 Rosi, A., Frodella, W., Nocentini, N., Caleca, F., Havenith, H.B., Strom, A., Saidov, M., Bimurzaev, G.A., and
705   Tofani, V.: Comprehensive landslide susceptibility map of Central Asia, Nat. Hazards Earth Syst. Sci., 23,
706   2229–2250, https://doi.org/10.5194/nhess-23-2229-2023, 2023.

707 Saponaro, A., Pilz, M., Wieland, M., Bindi, D., Moldobekov, B., and Parolai, S.: Landslide susceptibility analysis
708   in data-scarce regions: the case of Kyrgyz Republic. Bull. Eng. Geol. Environ. 74, 1117–1136, 2014.

709 Schlögel, R., Torgoev, I., De, Marneffe, C., and Havenith, H.B.: Evidence of a changing size-frequency
710   distribution of landslides in the Kyrgyz Tien Shan, Central Asia. Earth Surf Process Landf 36(12), 1658–
711   1669, 2011.

712 Schuster, R.L., and Evans, S.G.: Engineering Measures for the Hazard Reduction of Landslide Dams, in: Natural
713   and Artificial Rockslide Dams. Lecture Notes in Earth Sciences, edited by: Evans, S., Hermanns, R., Strom,

714   A., Scarascia-Mugnozza, G., Springer, Berlin, Heidelberg, https://doi.org/10.1007/978-3-642-04764-0_2,

715   2011.

716   Semakova, E., Gunasekara, K., and Semakov, D.: Identification of the glaciers and mountain naturally dammed

717   lakes in the Pskem, the Kashkadarya and the Surhandarya River basins, Uzbekistan, using ALOS satellite

718   data, Geomat. Nat. Hazards Risk, 7(3), 1081-1098, 2016.

719   Strom, A.: Landslide dams in Central Asia region. Journal of the Japan Landslide Society, 47(6), 309-324, 2010.

720   Strom, A., and Abdrakhmatov, K.: Large-Scale Rockslide Inventories: From the Kokomeren River Basin to the

721   Entire Central Asia Region (WCoE 2014–2017, IPL-106-2, in: Workshop on World Landslide Forum.

722   Springer, Cham, pp. 339–346, 2017.

723   Strom, A., and Abdrakhmatov. K.: Rockslides and rock avalanches of Central Asia: distribution, morphology, and

724   internal structure. Elsevier, 441pg. ISBN: 978-0-12-803204-6, 2018.

725   Swanson, F.J., Oyagi, N., and Tominaga, M.: Landslide dams in Japan, in: Landslide dams: processes, risk and

726   mitigation, vol 3, edited by: Schuster R.L., Geotech. Sp., ASCE, New York, 131–145, 1986.

727   Tacconi Stefanelli, C., Segoni, S., Casagli, N., and Catani, F.: Geomorphic indexing of landslide dams evolution,

728   Eng. Geol., 208, 1–10. https://doi.org/10.1016/j.enggeo.2016.04.024, 2016.

729   Tacconi Stefanelli, C., Vilímek, V., Emmer, A., and Catani, F.: Morphological analysis and features of the

730   landslide dams in the Cordillera Blanca, Peru, Landslides, 15(3), 507-521, https://doi.org/10.1007/s10346-

731   017-0909-5, 2018.

732   Tacconi Stefanelli, C., Casagli, N., and Catani, F.: Landslide damming hazard susceptibility maps: a new GIS-

733   based procedure for risk management, Landslides, 17, 1635-1648, https://doi.org/10.1007/s10346-020-

734   01395-6, 2020.

735   Trifonov, V.G., Makarov, V.I., and Scobelev, S.F.: The Talas-Fergana active right-slip faults. Ann Tectonicae

736   6:224–237, 1992.

737   Ullah, S., Bindi, D., Pilz, M., Danciu, L., Weatherill, G., Zuccolo, E., Anatoly Ischuk, A., Mikhailova, N.N.,

738   Abdrakhmatov, K., and Parolai, S. Probabilistic seismic hazard assessment for Central Asia. Annals of

739   Geophysics, 58(1), 2015.

740   Wang, X., Ding, Y., Liu, S., Jiang, L., Wu, K., Jiang, Z., and Guo, W.: Changes of glacial lakes and implications

741   in Tian Shan, central Asia, based on remote sensing data from 1990 to 2010, Environ. Res. Lett., 8(4),

742   044052, 2013.

743   Wang, D., Laffan, S.W., Liu, and Y., and Wu, L.: Morphometric characterization of landform from DEMs, Int. J.

744   Geogr. Inf. Sci., 24(2), 305–326, 2010.

745   Wood, J.: Geomorphometry in LandSerf. In: Hengl, T. and Reuter, H.I. [Eds.]: Geomorphometry: Concepts,

746   Software, Applications, Dev. Soil. Sci., 33, 333-349, 2009.

747   Zubovich, A. V., Wang, X. Q., Scherba, Y. G., Schelochkov, G. G., Reilinger, R., Reigber, C., Mosienko, O.,
748   Molnar, P., Michajljow, W., Makarov, V.I., Li, J., Kuzikov, S.I., Herring, T.A., Hamburger, M.W., Hager
749   B.H., Dang, Y., Bragin, V.D., and Beisenbaev, R.: GPS velocity field for the Tien Shan and surrounding
750   regions. Tectonics, 29(6), 2010.